

Nonlinear neoclassical two-fluid theory of response of tokamak plasma to resonant error-field

Richard Fitzpatrick

Citation: [Physics of Plasmas](#) **25**, 082513 (2018); doi: 10.1063/1.5043203

View online: <https://doi.org/10.1063/1.5043203>

View Table of Contents: <http://aip.scitation.org/toc/php/25/8>

Published by the [American Institute of Physics](#)

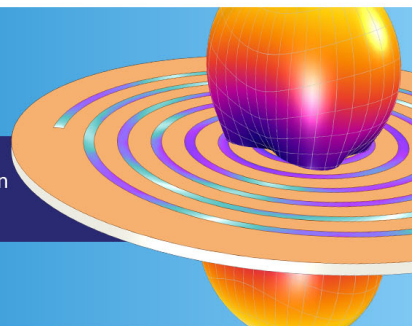
**COMSOL
CONFERENCE
2018 BOSTON**

Discover the power of multiphysics simulation.

COMSOL

OCTOBER 3-5
Boston Marriott Newton

Register Now ▶



Nonlinear neoclassical two-fluid theory of response of tokamak plasma to resonant error-field

Richard Fitzpatrick

Department of Physics, Institute for Fusion Studies, University of Texas at Austin, Austin, Texas 78712, USA

(Received 6 June 2018; accepted 31 July 2018; published online 17 August 2018)

A nonlinear, neoclassical, two-fluid theory of the interaction of a single-helicity magnetic island chain with a resonant error-field in a quasi-cylindrical, low- β , tokamak plasma is presented. In particular, the analysis of Fitzpatrick [Phys. Plasmas **25**, 042503 (2018)] is generalized to take explicit time dependence into account. Aside from the ability to more accurately treat time-varying problems, the main physical effect that is introduced into the theory by the incorporation of explicit time dependence is ion inertia. The formalism developed in the paper is used to analyze two time-varying problems. First, the interaction of a pre-existing magnetic island chain with a resonant error-field. Second, an error-field-maintained magnetic island chain. The latter problem is of direct relevance to experiments in which deliberately applied, multi-harmonic, resonant magnetic perturbations are used to suppress edge localized modes (ELMs) in tokamak plasmas. Indeed, the predictions of the theory are strikingly similar to data recently obtained from ELM suppression experiments in the DIII-D tokamak [R. Nazikian *et al.*, Nucl. Fusion **58**, 106010 (2018)]. *Published by AIP Publishing.* <https://doi.org/10.1063/1.5043203>

I. INTRODUCTION

Error-fields, resonant in the so-called *pedestal* region at the edge of the plasma, are sometimes deliberately applied to tokamak discharges in order to suppress edge localized modes (ELMs).^{1–4} Deliberately, the applied error-fields are usually referred to as resonant magnetic perturbations (RMPs). The mechanism by which RMPs suppress ELMs is not fully understood. It is thought that ELMs are triggered when the pedestal width exceeds a critical value.⁵ The most plausible working hypothesis is that the RMP generates a locked magnetic island chain just inside the top of the pedestal, inhibiting the growth of the pedestal width, and, thereby, maintaining the ELM-free state.⁶

The aim of this paper is to present a nonlinear, neoclassical, two-fluid theory of the interaction of a single-helicity magnetic island chain with a resonant error-field in a quasi-cylindrical, low- β , tokamak plasma. (The theory is “nonlinear” in the sense that it is an extension of the standard Rutherford island theory;^{7,8} it is “neoclassical” because it incorporates neoclassical ion and electron stress tensors; and it is “two-fluid” in the sense that the ion and electron fluid velocities are significantly different from one another due to diamagnetic flows.) The calculation is performed using a model that was developed, and gradually improved, in Refs. 9–19. The core of the model is a single-helicity version of the well-known four-field model of Hazeltine *et al.*²⁰ The core model is augmented by phenomenological terms representing anomalous cross-field particle and momentum transport due to small-scale plasma turbulence. Finally, the model includes approximate (i.e., flux-surface averaged) expressions for the divergences of the neoclassical ion and electron stress tensors. These expressions allow us to incorporate the bootstrap current, as well as neoclassical ion poloidal and perpendicular flow damping, into the analysis.

This paper presents an extension of the analysis presented in Ref. 19 that allows for explicit time dependence in the aforementioned nonlinear, neoclassical, two-fluid model. Aside from the ability to more accurately treat time-varying problems, the main physical effect that is introduced into the model by the incorporation of explicit time dependence is *ion inertia*.

II. PRELIMINARY ANALYSIS

A. Introduction

Consider a large aspect-ratio, low- β , circular cross-section, tokamak plasma equilibrium of major radius R_0 , and toroidal magnetic field-strength B_0 . Let us adopt a right-handed, quasi-cylindrical, toroidal coordinate system (r, θ, φ) whose symmetry axis ($r=0$) coincides with the magnetic axis. The coordinate r also serves as a label for the unperturbed (by the island chain) magnetic flux-surfaces. Let the equilibrium toroidal magnetic field and toroidal plasma current both run in the $+\varphi$ direction.

Suppose that a helical magnetic island chain, with m_0 poloidal periods, and n_φ toroidal periods, is embedded in the aforementioned plasma. The island chain is assumed to be radially localized in the vicinity of its associated rational surface, minor radius r_s , which is defined as the unperturbed magnetic flux-surface at which $q(r_s) = m_0/n_\varphi$. Here, $q(r)$ is the safety-factor profile. Let the full radial width of the island chain’s magnetic separatrix be $4w$. In the following, it is assumed that $r_s/R_0 \ll 1$ and $w/r_s \ll 1$.

The plasma is conveniently divided into an inner region that comprises the plasma in the immediate vicinity of the rational surface (and includes the island chain), and an outer region that comprises the remainder of the plasma. As is well known, a linear, marginally-stable, ideal-MHD analysis suffices to calculate the mode structure in the outer region.

Let us assume that the linear, marginally-stable, ideal-MHD solution has been found in the outer region. In the absence of an external perturbation, such a solution is characterized by a single real parameter, Δ' (with units of inverse length), known as the tearing stability index.²¹

B. Fundamental definitions

All fields in the inner region are assumed to depend on the normalized radial coordinate $X = (r - r_s)/w$ and the helical angle $\zeta = m_\theta \theta - n_\phi \phi - \phi_p(t)$, but may also depend explicitly on time, t . In particular, the electron number density, electron temperature, and ion temperature profiles in the inner region take the forms $n(X, \zeta, t) = n_0 (1 + \delta n/n_0)$, $T_e(X, \zeta, t) = T_{e0} (1 + \eta_e \delta n/n_0)$, $T_i(X, \zeta, t) = T_{i0} (1 + \eta_i \delta n/n_0)$, respectively. Here, n_0 , T_{e0} , T_{i0} , η_e , and η_i are uniform constants. Moreover, $(\partial/\partial X)[\delta n(X, \zeta, t)/n_0] \rightarrow -w/L_n$ as $|X| \rightarrow \infty$, where $L_n > 0$ is the density gradient scale-length at the rational surface. Note that we are assuming, for the sake of simplicity, that $\delta T_e/T_{e0} = \eta_e \delta n/n_0$, and $\delta T_i/T_{i0} = \eta_i \delta n/n_0$, where $\delta T_e = T_e - T_{e0}$. It follows that the flattening of the electron density profile within the magnetic separatrix of the island chain also implies the flattening of the electron and ion temperature profiles. Incidentally, the ion charge number is assumed to be unity.

It is convenient to define the poloidal wavenumber, $k_\theta = m_\theta/r_s$, the resonant safety-factor, $q_s = m_\theta/n_\phi$, the inverse aspect-ratio, $\epsilon_s = r_s/R_0$, the ion diamagnetic speed, $V_{*i} = T_{i0} (1 + \eta_i)/(e B_0 L_n)$, and the electron diamagnetic speed, $V_{*e} = \tau V_{*i}$, where $\tau = (T_{e0}/T_{i0}) [(1 + \eta_e)/(1 + \eta_i)]$, the poloidal ion gyroradius, $\rho_{\theta i} = (q_s/\epsilon_s) [T_{i0} (1 + \eta_i)/m_i]^{1/2} (m_i/e B_0)$, and the ion beta, $\beta_i = \mu_0 n_0 T_{i0} (1 + \eta_i)/B_0^2$. All of these quantities are evaluated at the rational surface. Here, e is the magnitude of the electron charge, and m_i is the ion mass.

C. Fundamental fields

The fundamental dimensionless fields in our nonlinear, neoclassical, two-MHD model are¹⁸ $\psi(X, \zeta, \hat{t}) = (q_s/\epsilon_s) \times (L_q/w) (A_\parallel/B_0 w)$, $N(X, \zeta, \hat{t}) = (L_n/w) (\delta n/n_0)$, $\phi(X, \zeta, \hat{t}) = -\Phi/(w B_0 V_{*i}) + v_p X$, $V(X, \zeta, \hat{t}) = (\epsilon_s/q_s) (V_{\parallel i}/V_{*i}) + v_p$, where $\hat{t} = k_\theta V_{*i} t$, $L_q = 1/(d \ln q/dr)_{r=r_s}$, $v_p(\hat{t}) = d\phi_p/d\hat{t}$. Here, A_\parallel is the component of the magnetic vector potential parallel to the equilibrium magnetic field (at the rational surface), $L_q > 0$ is the safety-factor gradient scale-length at the rational surface, Φ is the electric scalar potential, v_p is the normalized phase velocity of the island chain (in the laboratory frame), and $V_{\parallel i}$ is the component of the ion fluid velocity parallel to the equilibrium magnetic field (at the rational surface). The four fundamental fields are the normalized helical magnetic flux, the normalized perturbed electron number density, the normalized electric scalar potential, and the normalized parallel ion velocity, respectively.

D. Nonlinear neoclassical two-fluid model

In the inner region, our nonlinear, neoclassical, two-MHD model takes the form¹⁸

$$\frac{\partial_t(w^2 \psi)}{w^2} = [\phi + \tau N, \psi] + \eta J + \alpha_n^{-1} \hat{\nu}_{\theta e} [\alpha_n^{-1} J + V - \partial_X(\phi + \tau v_{\theta e} N) - v_{\theta i} - \tau v_{\theta e}], \quad (1)$$

$$\frac{\partial_t(w N)}{w} = [\phi, N] - \rho [\alpha_n V + J, \psi] - \alpha_c \rho [\phi + \tau N, X] + D \partial_X^2 N, \quad (2)$$

$$\partial_t V = [\phi, V] - \alpha_n (1 + \tau) [N, \psi] + \mu \partial_X^2 V - \hat{\nu}_{\theta i} [V - \partial_X(\phi - v_{\theta i} N)], \quad (3)$$

$$\frac{\epsilon \partial_t(w \partial_X^2 \phi)}{w} = \epsilon \partial_X [\phi - N, \partial_X \phi] + [J, \psi] + \alpha_c (1 + \tau) [N, X] + \epsilon \mu \partial_X^4 (\phi - N) + \hat{\nu}_{\theta i} \partial_X [V - \partial_X(\phi - v_{\theta i} N)] + \hat{\nu}_{\perp i} \partial_X [-\partial_X(\phi - v N)], \quad (4)$$

where

$$J = \beta^{-1} (\partial_X^2 \psi - 1), \quad (5)$$

and $[A, B] \equiv \partial_X A \partial_\zeta B - \partial_\zeta A \partial_X B$. Furthermore, $\partial_X \equiv (\partial/\partial X)_{\zeta, \hat{t}}$, $\partial_\zeta \equiv (\partial/\partial \zeta)_{X, \hat{t}}$, and $\partial_t \equiv (\partial/\partial \hat{t})_{X, \zeta}$. Here, Eq. (1) is the parallel Ohm's law, Eq. (2) the electron continuity equation, Eq. (3) the parallel ion equation of motion, and Eq. (4) the parallel ion vorticity equation. The auxiliary field $J(X, \zeta, \hat{t})$ is the normalized perturbed parallel current. Note that Eqs. (1)–(4) differ from the corresponding equations appearing in Ref. 19 due to the presence of terms involving explicit time dependence on the left-hand sides of the former equations.

The various dimensionless parameters appearing in Eqs. (1)–(5) have the following definitions:¹⁸ $\epsilon = (\epsilon_s/q_s)^2$, $\rho = (\rho_{\theta i}/w)^2$, $\alpha_n = (L_n/L_q) (w/\rho_{\theta i})^2$, $\alpha_c = 2(L_n/L_c) (w/\rho_{\theta i})^2$, $\beta = \beta_i (q_s/\epsilon_s)^2 (L_q/L_n)^2 (\rho_{\theta i}/w)^2$, $\eta = \beta \eta_\parallel / (\mu_0 k_\theta V_{*i} w^2)$,

$$D = \left[D_\perp + \beta_i (1 + \tau) \frac{\eta_\perp}{\mu_0} \left(1 - \frac{3}{2} \frac{\eta_e}{1 + \eta_e} \frac{\tau}{1 + \tau} \right) \right] \frac{1}{k_\theta V_{*i} w^2}, \quad (6)$$

$\mu = \mu_{\perp i} / (n_0 m_i k_\theta V_{*i} w^2)$, $\hat{\nu}_{\theta i} = (\epsilon_s/q_s)^2 [\nu_{\theta i} / (k_\theta V_{*i})]$, $\hat{\nu}_{\perp i} = (\epsilon_s/q_s)^2 [\nu_{\perp i} / (k_\theta V_{*i})]$, $\hat{\nu}_{\theta e} = (m_e/m_i) (\epsilon_s/q_s)^2 [\nu_{\theta e} / (k_\theta V_{*i})]$, $v_{\theta i} = 1 - 1.172 \eta_i / (1 + \eta_i)$, $v_{\perp i} = 1 - 2.367 \eta_i / (1 + \eta_i)$, $v_{\theta e} = 1 - 0.717 \eta_e / (1 + \eta_e)$, $v(\hat{t}) = v_{\perp i} - v_p(\hat{t})$. Here, m_e is the electron mass and L_c is the mean radius of curvature of magnetic field-lines at the rational surface. The mean curvature is assumed to be favorable (i.e., $L_c > 0$).

The quantities η_\parallel and η_\perp are the parallel and perpendicular plasma resistivities, respectively, whereas D_\perp is a phenomenological cross-flux-surface particle diffusivity (due to small-scale plasma turbulence), and $\mu_{\perp i}$ a phenomenological cross-flux-surface ion viscosity (likewise, due to small-scale turbulence). All four of these quantities are evaluated at the rational surface, and are assumed to be constant across the inner region.

The quantities $\nu_{\theta i}$, $\nu_{\perp i}$, and $\nu_{\theta e}$ are the poloidal ion, the perpendicular (i.e., “toroidal”¹⁸) ion, and the poloidal electron neoclassical flow damping rates, respectively.

E. External toroidal momentum source

Suppose that the plasma is subject to an external toroidal momentum source, due, for instance, to unbalanced neutral

beam injection. Let the source be such that, in the absence of the island chain, it increases the toroidal ion fluid velocity at the rational surface by $\Delta V_{\phi i}$. We can take this effect into account in our analysis by writing $v_{\perp i} \rightarrow v_{\perp i} - \Delta \hat{V}_{\phi i}$, where $\Delta \hat{V}_{\phi i} = (\epsilon_s/q_s) (\Delta V_{\phi i}/V_{*i})$. Thus, the definition of $v_{\perp i}$ generalizes to give $v_{\perp i} = 1 - 2.367 [\eta_i/(1 + \eta_i)] - \Delta \hat{V}_{\phi i}$.

F. Spatial boundary conditions

Equations (1)–(5) are subject to the boundary conditions¹⁸

$$\psi(X, \zeta, \hat{t}) \rightarrow \frac{1}{2} X^2 + \cos \zeta, \quad (7)$$

$$\partial_X N(X, \zeta, \hat{t}) \rightarrow -1, \quad (8)$$

$$\partial_X \phi(X, \zeta, \hat{t}) \rightarrow -v, \quad (9)$$

$$\partial_X V(X, \zeta, \hat{t}) \rightarrow 0, \quad (10)$$

as $|X| \rightarrow \infty$. Note that the fields $\psi(X, \zeta, \hat{t})$, $V(X, \zeta, \hat{t})$, and $J(X, \zeta, \hat{t})$ are even in X , whereas the fields $N(X, \zeta, \hat{t})$ and $\phi(X, \zeta, \hat{t})$ are odd. Of course, all fields are periodic in ζ with period 2π . The boundary conditions (8)–(10) differ slightly from the corresponding boundary conditions appearing in Ref. 19 because the former set of boundary conditions constrain the radial gradients of $N(X, \zeta, \hat{t})$, $\phi(X, \zeta, \hat{t})$, and $V(X, \zeta, \hat{t})$ a long way from the island chain, whereas the latter set constrain the actual values of these fields (which turns out to not be appropriate in a problem that incorporates explicit time dependence). In the time-independent limit, these two sets of boundary conditions are equivalent.

G. Island geometry

To the lowest order, we expect that¹⁸

$$\psi(X, \zeta, \hat{t}) = \Omega(X, \zeta) \equiv \frac{1}{2} X^2 + \cos \zeta \quad (11)$$

in the inner region. In fact, this result, which is known as the *constant- ψ approximation*, holds as long as $\beta \ll 1$. The contours of $\Omega(X, \zeta)$ map out the magnetic flux-surfaces of a helical magnetic island chain whose O-points are located at $X=0$ and $\zeta = \pi$, and whose X-points are located at $X=0$ and $\zeta = 0$. The magnetic separatrix corresponds to $\Omega = 1$, the region enclosed by the separatrix to $-1 \leq \Omega < 1$, and the region outside the separatrix to $\Omega > 1$.

H. Flux-surface average operator

The flux-surface average operator, $\langle \dots \rangle$, is defined as the annihilator of $[A, \Omega]$. In other words, $\langle [A, \Omega] \rangle = 0$, for any field $A(X, \zeta, \hat{t})$. It follows that

$$\langle A(s, \Omega, \zeta, \hat{t}) \rangle = \oint \frac{A(s, \Omega, \zeta, \hat{t})}{[2(\Omega - \cos \zeta)]^{1/2}} \frac{d\zeta}{2\pi} \quad (12)$$

for $1 \leq \Omega$, and

$$\langle A(s, \Omega, \zeta, \hat{t}) \rangle = \int_{\zeta_0}^{2\pi - \zeta_0} \frac{A(s, \Omega, \zeta, \hat{t}) + A(-s, \Omega, \zeta, \hat{t})}{2[2(\Omega - \cos \zeta)]^{1/2}} \frac{d\zeta}{2\pi} \quad (13)$$

for $-1 \leq \Omega < 1$. Here, $s = \text{sgn}(X)$ and $\zeta_0 = \cos^{-1}(\Omega)$, where $0 \leq \zeta_0 \leq \pi$.

It is helpful to define $\tilde{A} \equiv A - \langle A \rangle / \langle 1 \rangle$. It follows that $\langle \tilde{A} \rangle = 0$, for any field $A(X, \zeta, \hat{t})$. It is also easily demonstrated that $\langle [A, F(\Omega, \hat{t})] \rangle = 0$, for any flux-surface function $F(\Omega, \hat{t})$.

I. Asymptotic matching

Standard asymptotic matching between the inner and outer regions yields^{7,8,22} the *island width evolution equation*

$$0 = \Delta' r_s + 2 m_\theta \left(\frac{w_v}{w} \right)^2 \cos \phi_p + J_c \beta \frac{r_s}{w}, \quad (14)$$

and the *island phase evolution equation*

$$0 = -2 m_\theta \left(\frac{w_v}{w} \right)^2 \sin \phi_p + J_s \beta \frac{r_s}{w}, \quad (15)$$

where

$$J_c = -2 \int_{-\infty}^{\infty} J \cos \zeta dX \frac{d\zeta}{2\pi} = -4 \int_{-1}^{\infty} \langle J \cos \zeta \rangle d\Omega, \quad (16)$$

$$J_s = -2 \int_{-\infty}^{\infty} J \sin \zeta dX \frac{d\zeta}{2\pi} = -4 \int_{-1}^{\infty} \langle X [J, \Omega] \rangle d\Omega. \quad (17)$$

Note that we are assuming that the plasma is subject to a resonant error-field. Here, $4 w_v$ is the full radial width of the vacuum island chain (i.e., the island chain obtained by naively superimposing the vacuum error-field onto the unperturbed plasma equilibrium), and ϕ_p becomes the helical phase-shift between the true island chain and the vacuum island chain.

The first term on the right-hand side of Eq. (14) governs the intrinsic stability of the island chain. (The chain is intrinsically stable if $\Delta' < 0$, and vice versa.) The second term represents the effect of the error-field on island width evolution. The final term represents the effect of helical currents flowing in the inner region on island width evolution.

The first term on the right-hand side of Eq. (15) represents the electromagnetic locking torque exerted on the plasma in the inner region by the error-field. The second term represents the drag torque due to the combined effects of ion inertia, poloidal ion neoclassical flow damping, perpendicular ion neoclassical flow damping, and ion viscosity.

J. Expansion procedure

Equations (1)–(5) are solved, subject to the boundary conditions (7)–(10), via an expansion in two small parameters, Δ and δ , where $\Delta \ll \delta \ll 1$. The expansion procedure is as follows. First, the coordinates X and ζ are assumed to be $\mathcal{O}(\Delta^0 \delta^0)$. Next, some particular ordering scheme is adopted for the sixteen physics parameters $v_{\theta i}$, $v_{\theta e}$, v , τ , α_n , α_c , ϵ , ρ , β , $\hat{v}_{\theta i}$, $\hat{v}_{\perp i}$, $\hat{v}_{\theta e}$, η , D , μ , and ∂_t . The fields ψ , N , ϕ , V , and J are then expanded in the form $\psi(X, \zeta) = \sum_{i,j=0,\infty} \psi_{i,j}(X, \zeta)$, et cetera, where $\psi_{i,j} \sim \mathcal{O}(\Delta^i \delta^j)$. Finally, Eqs. (1)–(5) are solved order by order, subject to the boundary conditions (7)–(10).

The reasoning behind the expansion procedure is discussed in detail in Ref. 19.

III. FUNDAMENTAL ANALYSIS

A. Ordering scheme

The adopted ordering scheme is¹⁸

$$\Delta^0 \delta^0 : v_{\theta i}, v_{\theta e}, v, \tau, \alpha_n, \rho,$$

$$\Delta^0 \delta^1 : \alpha_c, \epsilon, \beta,$$

$$\Delta^1 \delta^0 : \hat{v}_{\theta i}, \hat{v}_{\perp i}, \hat{v}_{\theta e}, \eta, D, \mu, \partial_t.$$

This ordering scheme is suitable for a constant- ψ (i.e., $\beta \ll 1$), sonic¹¹ (i.e., $\alpha_n \sim 1$), magnetic island chain whose radial width is similar to the ion poloidal gyroradius (i.e., $\rho \sim 1$), and which is embedded in a large aspect-ratio (i.e., $\epsilon \ll 1$) tokamak plasma equilibrium with a relatively weak magnetic field-line curvature (i.e., $\alpha_c \ll 1$). The plasma temperature is assumed to be sufficiently high, and the plasma collisionality consequently sufficiently low, that the various ion and electron neoclassical flow damping timescales, as well as the timescale on which current diffuses across the island chain, are all very much longer than a typical diamagnetic rotation timescale (i.e., $\hat{v}_{\theta i}, \hat{v}_{\perp i}, \hat{v}_{\theta e}, \eta \ll 1$). The island chain is assumed to be sufficiently wide that the typical timescales on which density and momentum diffuse across the inner region are both very much longer than a typical diamagnetic rotation timescale (i.e., $D, \mu \ll 1$). Finally, the island chain is assumed to evolve on a timescale that is very much longer than a typical diamagnetic rotation timescale (i.e., $\partial_t \ll 1$).

B. Order $\Delta^0 \delta^0$

To order $\Delta^0 \delta^0$, Eqs. (1)–(5) yield

$$0 = [\phi_{0,0} + \tau N_{0,0}, \psi_{0,0}], \quad (18)$$

$$0 = [\phi_{0,0}, N_{0,0}] - \rho [\alpha_n V_{0,0} + J_{0,0}, \psi_{0,0}], \quad (19)$$

$$0 = [\phi_{0,0}, V_{0,0}] - \alpha_n (1 + \tau) [N_{0,0}, \psi_{0,0}], \quad (20)$$

$$0 = [J_{0,0}, \psi_{0,0}], \quad (21)$$

$$\partial_X^2 \psi_{0,0} = 1. \quad (22)$$

Equations (7), (11), and (22) give

$$\psi_{0,0} = \Omega(X, \zeta). \quad (23)$$

Equation (21) implies that

$$J_{0,0} = J_0(\Omega, \hat{t}), \quad (24)$$

where $J_0(\Omega, \hat{t})$ is an arbitrary flux-surface function.

Equations (8)–(10) and (18)–(20) can be satisfied if

$$\phi_{0,0} = s \phi_0(\Omega, \hat{t}), \quad (25)$$

$$N_{0,0} = s N_0(\Omega, \hat{t}), \quad (26)$$

$$V_{0,0} = V_0(\Omega, \hat{t}), \quad (27)$$

where $\phi_0(\Omega, \hat{t})$, $N_0(\Omega, \hat{t})$, and $V_0(\Omega, \hat{t})$ are arbitrary flux-surface functions. Note that, by symmetry, $\phi_0 = N_0 = 0$ inside the separatrix, which means that the electron number density and temperature profiles are flattened in this region. Let

$$M(\Omega, \hat{t}) = -\partial_\Omega \phi_0, \quad (28)$$

$$L(\Omega, \hat{t}) = -\partial_\Omega N_0. \quad (29)$$

Equations (8) and (9) yield

$$M(\infty, \hat{t}) = \frac{v}{\sqrt{2\Omega}}, \quad (30)$$

$$L(\infty, \hat{t}) = \frac{1}{\sqrt{2\Omega}}. \quad (31)$$

Again, by symmetry, $M=L=0$ inside the separatrix. Finally, Eq. (10) implies that

$$\partial_\Omega V_0(\infty, \hat{t}) = 0. \quad (32)$$

C. Order $\Delta^0 \delta^1$

To order $\Delta^0 \delta^1$, Eqs. (4) and (24)–(26) give

$$[J_{1,0}, \Omega] = -\epsilon \partial_X [\phi_0 - N_0, \partial_X \phi_0] - \alpha_c (1 + \tau) [N_0, |X|]. \quad (33)$$

It follows, with the aid of Eqs. (28) and (29), that¹⁸

$$J_{0,1} = \frac{\epsilon}{2} \partial_\Omega [(M - L) M] \tilde{X}^2 - \alpha_c (1 + \tau) L |\tilde{X}|. \quad (34)$$

Finally, it is easily demonstrated that $\langle X [J_0, \Omega] \rangle = \langle X [J_{0,1}, \Omega] \rangle = 0$.¹⁸ In other words, neither J_0 nor $J_{0,1}$ contribute to the sine integral, J_s [see Eq. (17)]. Thus, in order to calculate J_s , and, hence, to determine the phase velocity of the island chain [see Eq. (15)], we must expand to higher order. The higher-order expansion is also necessary to determine the unknown flux-surface functions, $J_0(\Omega, \hat{t})$, $M(\Omega, \hat{t})$, $L(\Omega, \hat{t})$, and $V_0(\Omega, \hat{t})$.

D. Order $\Delta^1 \delta^0$

To order $\Delta^1 \delta^0$, Eqs. (1)–(4) and (23)–(27) yield

$$\frac{\partial_t(w^2 \Omega)}{w^2} = [\phi_{1,0} + \tau N_{1,0}, \Omega] + \eta J_0 + \alpha_n^{-1} \hat{v}_{\theta e} [\alpha_n^{-1} J_0 + V_0 - s \partial_X (\phi_0 + \tau v_{\theta e} N_0) - v_{\theta i} - \tau v_{\theta e}], \quad (35)$$

$$\frac{s \partial_t(w N_0)}{w} = s [\phi_{1,0}, N_0] + s [\phi_0, N_{1,0}] - \rho [\alpha_n V_{1,0} + J_{1,0}, \Omega] + s D \partial_X^2 N_0, \quad (36)$$

$$\partial_t V_0 = [\phi_{1,0}, V_0] + s [\phi_0, V_{1,0}] - \alpha_n (1 + \tau) [N_{1,0}, \Omega] + \mu \partial_X^2 V_0 - \hat{v}_{\theta i} [V_0 - s \partial_X (\phi_0 - v_{\theta i} N_0)], \quad (37)$$

$$0 = [J_{1,0}, \Omega] + \hat{v}_{\theta i} \partial_X [V_0 - s \partial_X (\phi_0 - v_{\theta i} N_0)] + \hat{v}_{\perp i} \partial_X [-s \partial_X (\phi_0 - v N_0)]. \quad (38)$$

It follows from Eqs. (11), (28), (29), and (35) that

$$\begin{aligned}
[\phi_{1,0} + \tau N_{1,0}, \Omega] &= -(\eta + \alpha_n^{-2} \hat{\nu}_{\theta e}) J_0 + \frac{1}{w^2} \frac{dw^2}{d\hat{t}} \cos \zeta \\
&\quad - \alpha_n^{-1} \hat{\nu}_{\theta e} [V_0 + |X| (M + \tau v_{\theta e} L) \\
&\quad - v_{\theta i} - \tau v_{\theta e}], \quad (39)
\end{aligned}$$

from Eq. (36) that

$$\begin{aligned}
[-L \phi_{1,0} + M N_{1,0} - s \rho \alpha_n V_{1,0} - s \rho J_{1,0}, \Omega] \\
= \frac{\partial_t (w N_0)}{w} + D X \partial_\Omega (X \partial_\Omega N_0), \quad (40)
\end{aligned}$$

from Eq. (37) that

$$\begin{aligned}
[\partial_\Omega V_0 \phi_{1,0} + s M V_{1,0} - \alpha_n (1 + \tau) N_{1,0}, \Omega] \\
= \partial_t V_0 - \mu X \partial_\Omega (X \partial_\Omega V_0) + \hat{\nu}_{\theta i} [V_0 + |X| (M - v_{\theta i} L)], \quad (41)
\end{aligned}$$

and from Eq. (38) that

$$\begin{aligned}
[J_{1,0}, \Omega] &= -\hat{\nu}_{\theta i} \partial_X [V_0 + |X| (M - v_{\theta i} L)] \\
&\quad - \hat{\nu}_{\perp i} \partial_X [|X| (M - v L)]. \quad (42)
\end{aligned}$$

E. Determination of flux-surface functions

Given that $M=L=0$ within the magnetic separatrix (i.e., $-1 \leq \Omega < 1$), the flux-surface average of Eq. (42) implies that $\partial_\Omega V_0 = 0$ in this region. The flux-surface average of Eq. (41) then reveals that $V_0 = 0$ within the separatrix. The previous four equations also suggest that $\phi_{1,0} = N_{1,0} = V_{1,0} = J_{1,0} = 0$ in this region. Note, finally, that the viscous terms in Eqs. (40) and (41) require the continuity of N_0 and V_0 across the separatrix.

The flux-surface average of Eq. (39) yields

$$\begin{aligned}
J_0(\Omega, \hat{t}) &= \frac{1}{\eta} \left(\frac{1}{1 + \epsilon \nu_{\theta e} \tau_e} \right) \frac{1}{w^2} \frac{dw^2}{d\hat{t}} \frac{\langle \cos \zeta \rangle}{\langle 1 \rangle} \\
&\quad - \alpha_n \left(\frac{\epsilon \nu_{\theta e} \tau_e}{1 + \epsilon \nu_{\theta e} \tau_e} \right) \left(V_0 + \frac{M + \tau v_{\theta e} L}{\langle 1 \rangle} - v_{\theta i} - \tau v_{\theta e} \right), \quad (43)
\end{aligned}$$

where $\tau_e = \nu_e^{-1} = m_e / (n_0 e^2 \eta_{\parallel})$ is the electron collision time.

The flux-surface average of Eq. (40) gives

$$\frac{\partial_t (w N_0)}{w} - \frac{D \partial_\Omega (\langle X^2 \rangle \partial_\Omega N_0)}{\langle 1 \rangle} = 0. \quad (44)$$

This equation must be solved in the interval $1 \leq \Omega < \infty$ (recall that $N_0 = 0$ in the interval $-1 \leq \Omega < 1$), subject to the boundary conditions [see Eqs. (29) and (31)]

$$N_0(1, \hat{t}) = 0, \quad (45)$$

$$\partial_\Omega N_0(\infty, \hat{t}) = -\frac{1}{\sqrt{2\Omega}}. \quad (46)$$

The flux-surface average of Eq. (41) yields

$$\partial_t V_0 - \frac{\mu \partial_\Omega (\langle X^2 \rangle \partial_\Omega V_0)}{\langle 1 \rangle} = -\hat{\nu}_{\theta i} \left(V_0 + \frac{M - v_{\theta i} L}{\langle 1 \rangle} \right), \quad (47)$$

where $L = -\partial_\Omega N_0$. This equation must be solved in the interval $1 \leq \Omega < \infty$ (recall that $V_0 = 0$ in the interval $-1 \leq \Omega < 1$), subject to the boundary conditions [see Eq. (32)]

$$V_0(1, \hat{t}) = 0, \quad (48)$$

$$\partial_\Omega V_0(\infty, \hat{t}) = 0. \quad (49)$$

Finally, the flux-surface average of Eq. (42) gives

$$\partial_\Omega \{ \hat{\nu}_{\theta i} [V_0 + \langle X^2 \rangle (M - v_{\theta i} L)] + \hat{\nu}_{\perp i} \langle X^2 \rangle (M - v L) \} = 0. \quad (50)$$

Making use of the boundary conditions (30)–(32), the previous equation can be integrated to produce

$$\begin{aligned}
\hat{\nu}_{\theta i} [V_0 + \langle X^2 \rangle (M - v_{\theta i} L)] + \hat{\nu}_{\perp i} \langle X^2 \rangle (M - v L) \\
= \hat{\nu}_{\theta i} [V_0(\infty, \hat{t}) + v - v_{\theta i}]. \quad (51)
\end{aligned}$$

Hence, we deduce that

$$\begin{aligned}
M(\Omega, \hat{t}) &= -\left(\frac{\hat{\nu}_{\theta i}}{\hat{\nu}_{\theta i} + \hat{\nu}_{\perp i}} \right) \frac{[V_0(\Omega, \hat{t}) - V_0(\infty, \hat{t}) - v + v_{\theta i}]}{\langle X^2 \rangle} \\
&\quad + \left(\frac{\hat{\nu}_{\theta i} v_{\theta i} + \hat{\nu}_{\perp i} v}{\hat{\nu}_{\theta i} + \hat{\nu}_{\perp i}} \right) L(\Omega, \hat{t}). \quad (52)
\end{aligned}$$

F. Evaluation of cosine integral

According to Eqs. (11), (16), (24), (34), and (43)

$$J_c = J_i + J_b + J_p + J_g, \quad (53)$$

where

$$J_i = -\tau_R \frac{d(w/r_s)}{dt} \frac{1}{\beta r_s} \int_{-1}^{\infty} 8 \frac{\langle \cos \zeta \rangle^2}{\langle 1 \rangle} d\Omega, \quad (54)$$

$$J_b = \alpha_n \left(\frac{\epsilon \nu_{\theta e} \tau_e}{1 + \epsilon \nu_{\theta e} \tau_e} \right) \int_1^{\infty} 4 \left(V_0 + \frac{M + \tau v_{\theta e} L}{\langle 1 \rangle} \right) \langle \cos \zeta \rangle d\Omega, \quad (55)$$

$$J_p = \epsilon \int_{1-}^{\infty} \partial_\Omega [(M - L) M] \langle \tilde{X}^2 \tilde{X}^2 \rangle d\Omega, \quad (56)$$

$$J_g = -\alpha_c (1 + \tau) \int_1^{\infty} 2L \langle |\tilde{X}| \tilde{X}^2 \rangle d\Omega, \quad (57)$$

and $\tau_R = \mu_0 r_s^2 / [\eta_{\parallel} (1 + \epsilon \nu_{\theta e} \tau_e)]$ is the neoclassically reduced resistive evolution timescale at the rational surface.²³ Here, J_i , J_b , J_p , and J_g parameterize the effects of magnetic induction, the perturbed bootstrap current, the perturbed ion polarization current, and the magnetic field-line curvature, on the island width evolution, respectively.

G. Evaluation of sine integral

According to Eqs. (17), (42), and (51),

$$J_s = \hat{\nu}_{\theta i} \int_1^\infty 4(\langle 1 \rangle \langle X^2 \rangle - 1)(M - v_{\theta i} L) d\Omega \\ + \hat{\nu}_{\perp i} \int_1^\infty 4(\langle 1 \rangle \langle X^2 \rangle - 1)(M - v L) d\Omega. \quad (58)$$

H. Island width evolution equation

Making use of Eqs. (14) and (53)–(57), the island width evolution equation reduces to

$$I_i \tau_R \frac{d}{dt} \left(\frac{w}{r_s} \right) = \Delta' r_s + 2 m_0 \left(\frac{w_v}{w} \right)^2 \cos \phi_p \\ + \beta \frac{r_s}{w} \left[\alpha_n \left(\frac{\epsilon \nu_{\theta e} \tau_e}{1 + \epsilon \nu_{\theta e} \tau_e} \right) I_b + \epsilon I_p \right. \\ \left. - \alpha_c (1 + \tau) I_g \right], \quad (59)$$

where

$$I_i = \int_{-1}^\infty 8 \frac{\langle \cos \zeta \rangle^2}{\langle 1 \rangle} d\Omega, \quad (60)$$

$$I_b = \int_1^\infty 4 \left(V_0 + \frac{M + \tau v_{\theta e} L}{\langle 1 \rangle} \right) \langle \cos \zeta \rangle d\Omega, \quad (61)$$

$$I_p = \int_{1-}^\infty \partial_\Omega [(M - L) M] \langle \tilde{X}^2 \tilde{X}^2 \rangle d\Omega, \quad (62)$$

$$I_g = \int_1^\infty 2L \langle |\tilde{X}| \tilde{X}^2 \rangle d\Omega. \quad (63)$$

I. Island phase evolution equation

According to Eqs. (15) and (58), the island phase evolution equation takes the form

$$0 = -2 m_0 \left(\frac{w_v}{w} \right)^2 \sin \phi_p + \beta \frac{r_s}{w} (\hat{\nu}_{\theta i} I_\theta + \hat{\nu}_{\perp i} I_\perp), \quad (64)$$

where

$$I_\theta = \int_1^\infty 4(\langle 1 \rangle \langle X^2 \rangle - 1)(M - v_{\theta i} L) d\Omega, \quad (65)$$

$$I_\perp = \int_1^\infty 4(\langle 1 \rangle \langle X^2 \rangle - 1)(M - v L) d\Omega. \quad (66)$$

Note that

$$\frac{d\phi_p}{d\hat{t}} = v_{\perp i} - v(\hat{t}). \quad (67)$$

IV. INTERACTION OF PRE-EXISTING MAGNETIC ISLAND CHAIN WITH RESONANT ERROR-FIELD

A. Introduction

Consider the interaction of a pre-existing magnetic island chain (i.e., an island chain that would be present in the absence of the error-field) with a resonant error-field. In the

following analysis, it is assumed that the pre-existing island chain's width evolves on a much longer timescale than that associated with its phase evolution. In other words, $\tau_R w/r_s \gg m_0/(k_\theta V_{*i} |v_{\perp i} - v_{\theta i}|)$. (This is a realistic assumption because the resistive timescale, τ_R , is generally much longer than any other relevant timescale in a high temperature tokamak plasma.) In this case, it is reasonable to assume that the chain's width remains approximately constant as its phase changes in time. [In fact, the relative magnitude of the phase-induced modulations in the island width is of the order $m_0/(k_\theta V_{*i} |v_{\perp i} - v_{\theta i}| \tau_R w/r_s) \ll 1$.]

B. Density profile

The density profile in the vicinity of the island chain, $N_0(\Omega, \bar{t})$, where $\bar{t} = D\hat{t}$, is determined by Eqs. (44)–(46), which can be written

$$\frac{\partial N_0}{\partial \bar{t}} - \frac{\partial_\Omega (\langle X^2 \rangle \partial_\Omega N_0)}{\langle 1 \rangle} = \frac{d \ln w}{d\bar{t}} N_0, \quad (68)$$

$$N_0(1, \bar{t}) = 0, \quad (69)$$

$$\partial_\Omega N_0(\infty, \bar{t}) = -\frac{1}{\sqrt{2\Omega}}. \quad (70)$$

Suppose that

$$\left| \frac{d \ln w}{d\bar{t}} \right| = \frac{1}{D} \left| \frac{d \ln w}{d\hat{t}} \right| \ll 1, \quad (71)$$

which implies that $D \gg \epsilon_R$, where $\epsilon_R \ll 1$ is defined in Eq. (173). In other words, suppose that the island chain's width evolves on a timescale that is much longer than that required for density to diffuse across the inner region. In this case, Eqs. (68)–(70) possess the obvious solution $N_0(\Omega, \bar{t}) = N_0(\Omega)$, where

$$N_0(\Omega) = -\int_1^\Omega \frac{d\Omega'}{\langle X^2 \rangle(\Omega')}. \quad (72)$$

Thus, it follows from Eq. (29) that $L = L(\Omega)$, where

$$L(\Omega) = \frac{1}{\langle X^2 \rangle}. \quad (73)$$

C. Derivation of island phase evolution equations

Let $T = |v_{\perp i} - v_{\theta i}| \hat{t}$, $\bar{\nu} = \hat{\nu}_{\perp i} / \hat{\nu}_{\theta i}$, $\bar{\mu} = \mu / \hat{\nu}_{\theta i}$, $\gamma = |v_{\perp i} - v_{\theta i}| / \hat{\nu}_{\theta i}$, and $\phi'_p = s_i \phi_p$, where $s_i = \text{sgn}(v_{\perp i} - v_{\theta i})$. Note that if $s_i > +1$ then, in the absence of the error-field, the island chain rotates in the electron diamagnetic direction (in the laboratory frame). On the other hand, if $s_i = -1$ then the island chain rotates in the ion diamagnetic direction. In fact, the island chain's so-called *natural frequency*²² of rotation is $d\phi_p/dt = \omega_0$, where

$$\omega_0 = k_\theta V_{*i} (v_{\perp i} - v_{\theta i}). \quad (74)$$

This frequency should be compared to

$$\omega_{\perp e} = k_{\theta} V_{*i} (v_{\perp i} + \tau), \quad (75)$$

$$\omega_E = k_{\theta} V_{*i} v_{\perp i}, \quad (76)$$

$$\omega_{\perp i} = k_{\theta} V_{*i} (v_{\perp i} - 1), \quad (77)$$

which are the natural frequencies calculated on the assumption that the island chain is convected by the electron fluid, rotates at the $\mathbf{E} \times \mathbf{B}$ velocity, and is convected by the ion fluid, respectively. It follows that

$$\omega_0 - \omega_E = -k_{\theta} V_{*i} v_{\theta i} = -k_{\theta} V_{*i} \left(\frac{1 - 0.172 \eta_i}{1 + \eta_i} \right). \quad (78)$$

Hence, we deduce that $\omega_0 - \omega_E < 0$ for $\eta_i < 5.81$, which implies that the natural frequency lies between ω_E and $\omega_{\perp i}$ (unless η_i is very large), as is generally observed in experiments.^{24,25}

It is convenient to write

$$v(T) = v_{\theta i} + (v_{\perp i} - v_{\theta i}) \left(1 - \frac{d\phi'_p}{dT} \right), \quad (79)$$

$$V_0(\Omega, T) = \bar{V}_0(\Omega) + (v_{\perp i} - v_{\theta i}) v_0(\Omega, T), \quad (80)$$

$$M(\Omega, T) = \bar{M}(\Omega) + (v_{\perp i} - v_{\theta i}) m(\Omega, T). \quad (81)$$

It follows from Eqs. (52), (67), and (73) that

$$\bar{M}(\Omega) = - \left(\frac{1}{1 + \bar{\nu}} \right) \frac{[\bar{V}_0(\Omega) - \bar{V}_0(\infty)]}{\langle X^2 \rangle} + \frac{v_{\theta i}}{\langle X^2 \rangle}, \quad (82)$$

$$m(\Omega, T) = - \left(\frac{1}{1 + \bar{\nu}} \right) \frac{[v_0(\Omega, T) - v_0(\infty, T)]}{\langle X^2 \rangle} + \frac{1 - d\phi'_p/dT}{\langle X^2 \rangle}. \quad (83)$$

Hence, Eqs. (47)–(49) yield

$$f(\Omega) \bar{V}_0(\Omega) - \frac{\bar{\mu} d_{\Omega} [\langle X^2 \rangle d_{\Omega} \bar{V}_0(\Omega)]}{\langle 1 \rangle} = - \left(\frac{1}{1 + \bar{\nu}} \right) \frac{\bar{V}_0(\infty)}{\langle 1 \rangle \langle X^2 \rangle}, \quad (84)$$

where

$$\bar{V}_0(1) = d_{\Omega} \bar{V}_0(\infty) = 0 \quad (85)$$

and

$$f(\Omega) = 1 - \left(\frac{1}{1 + \bar{\nu}} \right) \frac{1}{\langle 1 \rangle \langle X^2 \rangle}. \quad (86)$$

Here, $d_{\Omega} \equiv d/d\Omega$. The previous three equations possess the obvious solution

$$\bar{V}_0(\Omega) = 0. \quad (87)$$

Thus, it follows from Eq. (82) that

$$\bar{M}(\Omega) = \frac{v_{\theta i}}{\langle X^2 \rangle}. \quad (88)$$

Equations (47)–(49) also yield

$$\begin{aligned} \gamma \frac{\partial v_0(\Omega, T)}{\partial T} + f(\Omega) v_0(\Omega, T) - \frac{\bar{\mu} d_{\Omega} [\langle X^2 \rangle \partial_{\Omega} v_0(\Omega, T)]}{\langle 1 \rangle} \\ = - \left(\frac{1}{1 + \bar{\nu}} \right) \frac{v_0(\infty, T)}{\langle 1 \rangle \langle X^2 \rangle} - \frac{1 - d\phi'_p/dT}{\langle 1 \rangle \langle X^2 \rangle}, \end{aligned} \quad (89)$$

where

$$v_0(1, T) = \partial_{\Omega} v_0(\infty, T) = 0. \quad (90)$$

Furthermore, Eqs. (64)–(66) can be combined with the previous analysis contained in this section to give

$$\begin{aligned} \left[\frac{2 m_{\theta} w_v^2}{\beta |v_{\perp i} - v_{\theta i}| \hat{v}_{\theta i} r_s w} \right] \sin \phi'_p \\ = \int_1^{\infty} \frac{4 (\langle 1 \rangle \langle X^2 \rangle - 1)}{\langle X^2 \rangle} \times \left[-v_0(\Omega, T) + v_0(\infty, T) \right. \\ \left. + 1 - \frac{d\phi'_p}{dT} \right] d\Omega. \end{aligned} \quad (91)$$

Equations (86), (89), and (90) imply that

$$\gamma \frac{\partial v_0(\infty, T)}{\partial T} + v_0(\infty, T) = - \left(1 - \frac{d\phi'_p}{dT} \right). \quad (92)$$

Here, we have made use of the fact that $\langle 1 \rangle \langle X^2 \rangle \rightarrow 1$ as $\Omega \rightarrow \infty$. Hence

$$v_0(\infty, T) = -1 + \frac{1}{\gamma} \int_{-\infty}^T e^{(T-T')/\gamma} \frac{d\phi'_p}{dT'} dT', \quad (93)$$

and Eqs. (89) and (91) yield

$$\begin{aligned} \gamma \frac{\partial v_0}{\partial T} + f(\Omega) v_0 - \frac{\bar{\mu} d_{\Omega} [\langle X^2 \rangle \partial_{\Omega} v_0]}{\langle 1 \rangle} \\ = - \frac{1}{\langle 1 \rangle \langle X^2 \rangle} \left[\frac{\bar{\nu}}{1 + \bar{\nu}} - \frac{d\phi'_p}{dT} \right. \\ \left. + \frac{1}{1 + \bar{\nu}} \frac{1}{\gamma} \int_{-\infty}^T e^{(T-T')/\gamma} \frac{d\phi'_p}{dT'} dT' \right], \end{aligned} \quad (94)$$

$$\begin{aligned} \left[\frac{2 m_{\theta} w_v^2}{\beta |v_{\perp i} - v_{\theta i}| \hat{v}_{\theta i} r_s w} \right] \sin \phi'_p \\ = \int_1^{\infty} \frac{4 (\langle 1 \rangle \langle X^2 \rangle - 1)}{\langle X^2 \rangle} \times \left[-v_0 - \frac{d\phi'_p}{dT} \right. \\ \left. + \frac{1}{\gamma} \int_{-\infty}^T e^{(T-T')/\gamma} \frac{d\phi'_p}{dT'} dT' \right] d\Omega, \end{aligned} \quad (95)$$

respectively. However, successive integration by parts reveals that

$$\frac{1}{\gamma} \int_{-\infty}^T e^{(T-T')/\gamma} \frac{d\phi'_p}{dT'} dT' = \frac{d\phi'_p}{dT} + \sum_{n=2, \infty} (-\gamma)^{n-1} \frac{d^n \phi'_p}{dT^n}. \quad (96)$$

Thus, we arrive at the following closed set of equations that govern the phase evolution of the island chain:

$$\begin{aligned} \gamma \frac{\partial v_0}{\partial T} + f(\Omega) v_0 - \frac{\bar{\mu} \partial_\Omega [\langle X^2 \rangle \partial_\Omega v_0]}{\langle 1 \rangle} \\ = -\frac{1}{(1 + \bar{\nu}) \langle 1 \rangle \langle X^2 \rangle} \left[\bar{\nu} \left(1 - \frac{d\phi'_p}{dT} \right) \right. \\ \left. + \sum_{n=2, \infty} (-\gamma)^{n-1} \frac{d^n \phi'_p}{dT^n} \right], \end{aligned} \quad (97)$$

$$v_0(1, T) = \partial_\Omega v_0(\infty, T) = 0, \quad (98)$$

$$\begin{aligned} \left[\frac{2m_\theta w_v^2}{\beta |v_{\perp i} - v_{\theta i}| \hat{v}_{\theta i} r_s w} \right] \sin \phi'_p \\ = \int_1^\infty \frac{4 \langle 1 \rangle \langle X^2 \rangle - 1}{\langle X^2 \rangle} \times \left[-v_0 + \sum_{n=2, \infty} (-\gamma)^{n-1} \frac{d^n \phi'_p}{dT^n} \right] d\Omega. \end{aligned} \quad (99)$$

D. Inviscid limit

Suppose that the term involving the normalized ion viscosity, $\bar{\mu}$, can be neglected in Eq. (97). As explained in Ref. 18, this approximation is valid provided that $\bar{\mu} \ll 1$, $\sqrt{\bar{\nu}}$. It follows that

$$\begin{aligned} v_0(\Omega, T) = -\frac{1}{(1 + \bar{\nu}) \langle 1 \rangle \langle X^2 \rangle f} \\ \times \left[\bar{\nu} - \bar{\nu} \frac{f}{\gamma} \int_{-\infty}^T e^{(T-T')(f/\gamma)} \frac{d\phi'_p}{dT'} dT' \right. \\ \left. + \sum_{n=2, \infty} (-\gamma)^{n-1} \frac{f}{\gamma} \int_{-\infty}^T e^{(T-T')(f/\gamma)} \frac{d^n \phi'_p}{dT'^n} dT' \right]. \end{aligned} \quad (100)$$

Note that this expression automatically satisfies the boundary conditions (98), because $\langle 1 \rangle \langle X^2 \rangle \rightarrow \infty$ as $\Omega \rightarrow 1$, and $\langle 1 \rangle \langle X^2 \rangle \rightarrow 1$ as $\Omega \rightarrow \infty$. However, successive integration by parts yields

$$\begin{aligned} v_0(\Omega, T) = -\frac{1}{(1 + \bar{\nu}) \langle 1 \rangle \langle X^2 \rangle f} \left[\bar{\nu} \left(1 - \frac{d\phi'_p}{dT} \right) \right. \\ \left. + \sum_{n=2, \infty} (-\gamma)^{n-1} \left(\sum_{m=0, n-2} \frac{1}{f^m} - \frac{\bar{\nu}}{f^{n-1}} \right) \frac{d^n \phi'_p}{dT^n} \right]. \end{aligned} \quad (101)$$

The previous expression can be combined with Eq. (99) to produce the following ordinary differential equation that governs the time evolution of the island phase:

$$\lambda_v \sin \phi'_p = 1 - \frac{d\phi'_p}{dT} - \sum_{n=2, \infty} (-1)^n \Gamma_{n-1} \frac{d^n \phi'_p}{dT^n}, \quad (102)$$

where

$$\lambda_v = \frac{2m_\theta w_v^2}{I_v \beta |v_{\perp i} - v_{\theta i}| \hat{v}_{\theta i} r_s w}, \quad (103)$$

$$I_v = \frac{\bar{\nu}}{1 + \bar{\nu}} \int_1^\infty \frac{4 \langle 1 \rangle \langle X^2 \rangle - 1}{\langle 1 \rangle \langle X^2 \rangle^2 f} d\Omega, \quad (104)$$

$$\Gamma_n = \frac{\gamma^n}{I_v} \int_1^\infty \frac{4 \langle 1 \rangle \langle X^2 \rangle - 1}{\langle 1 \rangle \langle X^2 \rangle^2 f^{n+1}} d\Omega. \quad (105)$$

We can identify the various terms that appear in the inviscid island phase evolution equation, (102). The term on the left-hand side represents the electromagnetic locking torque due to the error-field; the first term on the right-hand side represents intrinsic plasma rotation, the second term represents ion neoclassical flow damping, and the final term represents ion inertia.

Let $k = [(1 + \Omega)/2]^{1/2}$. It follows that

$$I_v = \frac{\bar{\nu}}{1 + \bar{\nu}} \int_1^\infty \frac{8(\mathcal{A}\mathcal{C} - 1)}{\mathcal{A}\mathcal{C}^2 f} dk, \quad (106)$$

$$\Gamma_n = \gamma^n \left(\frac{1 + \bar{\nu}}{\bar{\nu}} \right) \int_1^\infty \frac{8(\mathcal{A}\mathcal{C} - 1)^2}{\mathcal{A}\mathcal{C}^2 f^{n+1}} dk / \int_1^\infty \frac{8(\mathcal{A}\mathcal{C} - 1)}{\mathcal{A}\mathcal{C}^2 f} dk, \quad (107)$$

where $\mathcal{A}(k)$ and $\mathcal{C}(k)$ are defined in the Appendix, and

$$f(k) = 1 - \frac{1}{1 + \bar{\nu}} \frac{1}{\mathcal{A}\mathcal{C}}. \quad (108)$$

Thus, in the limit $\bar{\nu} \gg 1$, we obtain

$$I_v = \int_1^\infty \frac{8(\mathcal{A}\mathcal{C} - 1)}{\mathcal{A}\mathcal{C}^2} dk = I_{v\infty}, \quad (109)$$

$$\Gamma_n = \gamma^n \int_1^\infty \frac{8(\mathcal{A}\mathcal{C} - 1)^2}{\mathcal{A}\mathcal{C}^2} dk / \int_1^\infty \frac{8(\mathcal{A}\mathcal{C} - 1)}{\mathcal{A}\mathcal{C}^2} dk = C_\infty \gamma^n, \quad (110)$$

where $I_{v\infty} = 3.5724 \times 10^{-1}$ and $C_\infty = 1.8182 \times 10^{-1}$. In the opposite limit, $\bar{\nu} \ll 1$, we get

$$I_v = \bar{\nu}^{3/4} \frac{4}{2^{1/4}} \int_0^\infty \frac{dx}{1 + x^4} = I_{v0} \bar{\nu}^{3/4}, \quad (111)$$

$$\Gamma_n = \left(\frac{\gamma}{\bar{\nu}} \right)^n \int_0^\infty \frac{(x^4)^{n-1}}{(1 + x^4)^{n+1}} dx / \int_0^\infty \frac{dx}{1 + x^4} = C_n \left(\frac{\gamma}{\bar{\nu}} \right)^n. \quad (112)$$

Here, $I_{v0} = 2^{1/4} \pi$, and²⁶

$$C_n = \frac{\sqrt{8} \Gamma(7/4) \Gamma(n + 1/4)}{\pi (4n - 3) \Gamma(n + 1)}, \quad (113)$$

where $\Gamma(x)$ is a gamma function. Note that the C_n are all positive, and are decreasing functions of n . In particular, $C_1 = 3/4$. Incidentally, the results (111) and (112) follow because $\mathcal{A}\mathcal{C} \rightarrow 1 + 1/(32k^4)$ as $k \rightarrow \infty$.

E. Locked solutions

Let us search for the so-called *locked* solutions of the inviscid island phase evolution equation, (102), in which the island phase, ϕ'_p , is independent of time. It is clear that if $d^n \phi'_p / dT^n = 0$ for all $n > 0$, then Eq. (102) reduces to

$$\lambda_v \sin \phi'_p = 1. \quad (114)$$

This equation is only soluble if the so-called *locking parameter*, λ_v , exceeds the critical value unity. In this case, the two possible solutions are

$$\phi'_p = \sin^{-1}\left(\frac{1}{\lambda_v}\right) \quad (115)$$

and

$$\phi'_p = \pi - \sin^{-1}\left(\frac{1}{\lambda_v}\right), \quad (116)$$

where $-\pi/2 \leq \sin^{-1}x \leq \pi/2$. In the first case, the island chain locks in a destabilizing phase relation with respect to the error-field [i.e., $\cos \phi'_p = \cos \phi_p > 0$; see Eq. (59)]. In the second, the island chain locks in the stabilizing phase relation with respect to the error-field (i.e., $\cos \phi'_p < 0$).

Let us investigate the stability of the two locked solutions. For the first solution, we can write

$$\phi'_p(T) = \sin^{-1}\left(\frac{1}{\lambda_v}\right) + \delta\phi'_p e^{-pT}. \quad (117)$$

Likewise, for the second solution, we can write

$$\phi'_p(T) = \pi - \sin^{-1}\left(\frac{1}{\lambda_v}\right) + \delta\phi'_p e^{-pT}. \quad (118)$$

Substituting into Eq. (102), and then linearizing, we obtain

$$s_v \sqrt{\lambda_v^2 - 1} = p - \sum_{n=2, \infty} \Gamma_{n-1} p^n, \quad (119)$$

where $s_v = +1$ for the first solution, and $s_v = -1$ for the second.

Consider the high perpendicular ion neoclassical flow damping limit, $\bar{\nu} \gg 1$. It follows from Eqs. (110) and (119) that

$$\epsilon_v = q - C_\infty \sum_{n=2, \infty} q^n, \quad (120)$$

where $q = \gamma p$, and

$$\epsilon_v = s_v \gamma \sqrt{\lambda_v^2 - 1}. \quad (121)$$

Given that $\sum_{n=2, \infty} q^n = q^2/(1-q)$, provided $|q| < 1$, Eq. (120) can be written in the form

$$\epsilon_v = F(q), \quad (122)$$

where

$$F(q) = q - C_\infty \left(\frac{q^2}{1-q} \right). \quad (123)$$

Figure 1 shows the function $F(q)$. A given solution is stable if the corresponding roots of Eq. (122) are all such that $q > 0$, and unstable otherwise. It is clear, from the figure, that the solution in which the island chain locks in a

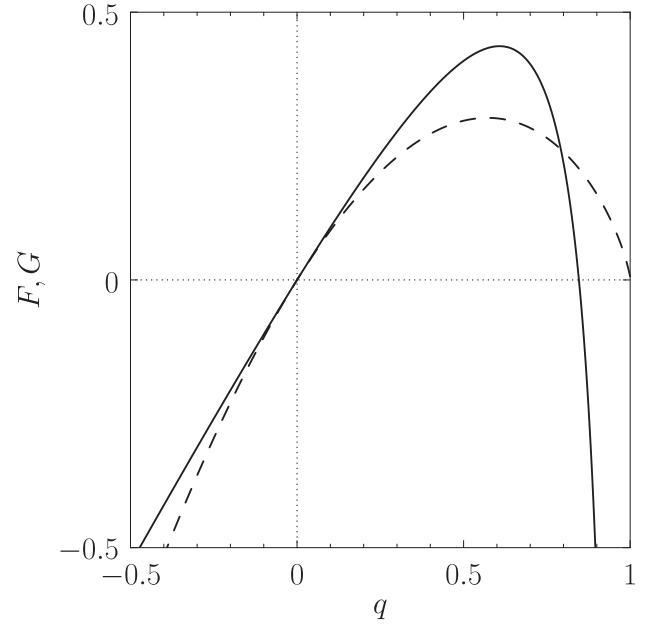


FIG. 1. Stability of locked solutions of the inviscid island phase evolution equation for the case of a pre-existing island chain interacting with a resonant error-field. The solid curve shows the function $F(q)$, defined in Eq. (123). The dashed curve shows the function $G(q)$ defined in Eq. (126).

destabilizing phase relation with respect to the error-field (i.e., $\epsilon_v > 0$) is stable, whereas the solution in which the chain locks in a stabilizing phase relation (i.e., $\epsilon_v < 0$) is unstable.

Consider the low perpendicular ion neoclassical flow damping limit, $\bar{\nu} \ll 1$. It follows from Eqs. (112), (113), and (119) that

$$\epsilon_v = G(q), \quad (124)$$

where $q = (\gamma/\bar{\nu})p$, and

$$\epsilon_v = s_v \frac{\gamma}{\bar{\nu}} \sqrt{\lambda_v^2 - 1}, \quad (125)$$

with

$$G(q) = q - \sum_{n=2, \infty} \frac{\sqrt{8} \Gamma(7/4) \Gamma(n-3/4) q^n}{\pi (4n-7) \Gamma(n)}. \quad (126)$$

Figure 1 shows the function $G(q)$. Now, a given solution is stable if $q > 0$, and unstable otherwise. It is again clear that the solution in which the island chain locks in a destabilizing phase relation with respect to the error-field (i.e., $\epsilon_v > 0$) is stable, whereas the solution in which the chain locks in a stabilizing phase relation (i.e., $\epsilon_v < 0$) is unstable.

In conclusion, a stable locked solution is possible provided $\lambda_v > 1$. The solution is such that $\sin \phi'_p = 1/\lambda_v$ and $\cos \phi'_p = \sqrt{\lambda_v^2 - 1}/\lambda_v$. It follows that the island chain always locks to the error-field in a destabilizing phase relation.²²

F. Rotating solutions

Let us now consider the so-called *rotating* solutions of the inviscid island phase evolution equation, (102), in which

the island phase, ϕ'_p , varies in time. Such solutions are more difficult to find than locked solutions because of the highly nonlinear nature of the left-hand side of Eq. (102). However, progress can be made by treating the ion inertia parameter, γ , as a small quantity (i.e., $\gamma \ll 1$).

Neglecting terms in Eq. (102) that are $\mathcal{O}(\gamma^2)$ or smaller, we obtain

$$\Gamma_1 \frac{d^2 \phi'_p}{dT^2} + \frac{d\phi'_p}{dT} + \lambda_v \sin \phi'_p \simeq 1. \quad (127)$$

To the lowest order in γ ,

$$\frac{d\phi'_p}{dT} = 1 - \lambda_v \sin \phi'_p, \quad (128)$$

which implies that

$$\frac{d^2 \phi'_p}{dT^2} = -\lambda_v \cos \phi'_p \frac{d\phi'_p}{dT}. \quad (129)$$

Hence, to the first order in Γ_1 , we get

$$\frac{d\phi'_p}{dT} = \frac{1 - \lambda_v \sin \phi'_p}{1 - \Gamma_1 \lambda_v \cos \phi'_p}. \quad (130)$$

The normalized rotation period of the island chain takes the form²⁷

$$\begin{aligned} \tau_p &= \oint \frac{dT}{d\phi'_p} d\phi'_p = \oint \frac{1 - \Gamma_1 \sin y}{1 + \lambda_v \cos y} dy \\ &= \oint \frac{dy}{1 + \lambda_v \cos y} = \frac{2\pi}{\sqrt{1 - \lambda_v^2}}. \end{aligned} \quad (131)$$

Note that the rotation period goes to infinity as the locking parameter approaches the critical value unity; this result indicates that only locked solutions exist for $\lambda_v > 1$. Furthermore, the rotation period is independent of the effective ion inertia parameter, Γ_1 .

Equation (130) can be integrated to give²⁸

$$\begin{aligned} \frac{T}{\tau_p} &= \frac{1}{\pi} \tan^{-1} \left[\left(\frac{1 + \lambda_v}{1 - \lambda_v} \right)^{1/2} \tan \left(\frac{\phi'_p}{2} - \frac{\pi}{4} \right) \right] \\ &+ \Gamma_1 \frac{\sqrt{1 - \lambda_v^2}}{2\pi} \log \left(\frac{1 - \lambda_v \sin \phi'_p}{1 - \lambda_v} \right), \end{aligned} \quad (132)$$

assuming that $T=0$ when $\phi'_p = \pi/2$. Figures 2–4 illustrate the typical time evolution of the island phase predicted by the previous expression. (We have adopted unrealistically large values of γ in order to make the effect of ion inertia more apparent in these figures.) It can be seen that as the locking parameter, λ_v , increases toward the critical value unity, the island rotation becomes more and more uneven, because the electromagnetic locking torque causes the rotation to slow down when $\sin \phi'_p > 0$ and to speed up when $\sin \phi'_p < 0$. However, in the absence of ion inertia (i.e., $\Gamma_1 = 0$), the island chain spends as much time having a stabilizing phase relation with respect to the error-field (i.e.,

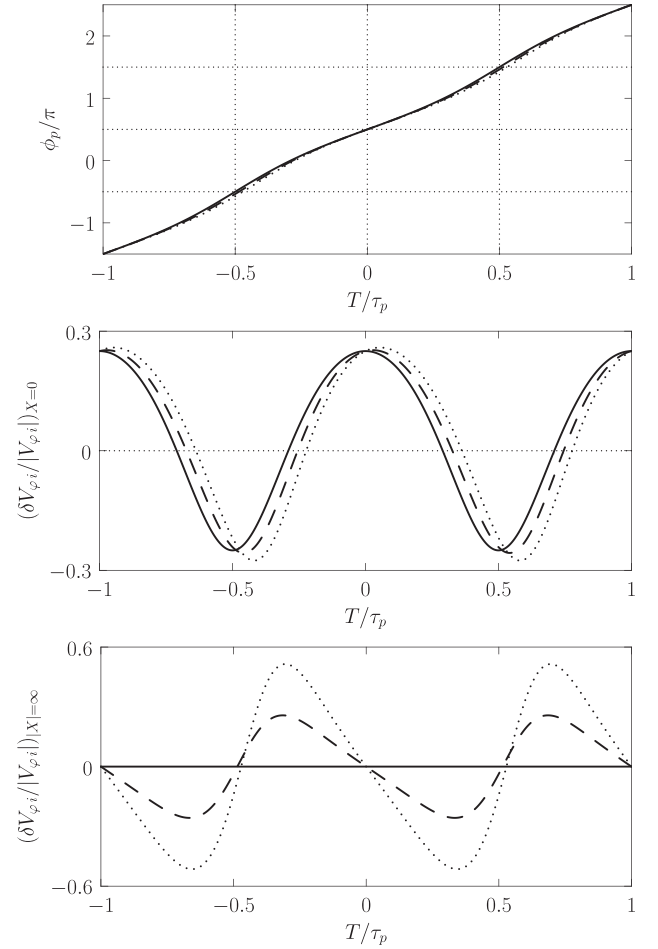


FIG. 2. Time evolution of a rotating pre-existing island chain interacting with a resonant error-field. The solid, dashed, and dotted curves are calculated with $\lambda_v = 0.25$ and $\gamma = 0.0, 1.0$, and 2.0 , respectively. The top, middle, and bottom panels show the island phase, the perturbed toroidal ion fluid velocity inside the separatrix, and the perturbed toroidal ion fluid velocity many island widths distant from the separatrix, respectively. The natural frequency is in the electron diamagnetic direction (i.e., $s_i = +1$). The calculation is made in the large perpendicular ion neoclassical flow damping limit, $\bar{\nu} \gg 1$, in which $\Gamma_1 = 0.18182\gamma$.

$\cos \phi'_p < 0$) as it does having a destabilizing phase relation (i.e., $\cos \phi'_p > 0$). On the other hand, in the presence of ion inertia (i.e., $\Gamma_1 > 0$), the island chain spends slightly more time having a stabilizing phase relation with respect to the error-field than it does having a destabilizing phase relation.²²

The toroidal ion fluid velocity is given by

$$\frac{\epsilon_s}{q_s} \frac{V_{\phi i}(\Omega, T)}{V_{*i}} = (v_{\perp i} - v_{\theta i}) \left[-\frac{d\phi'_p}{dT} + v_0(\Omega, T) \right]. \quad (133)$$

However, Eqs. (93) and (96) reveal that, to the first order in the ion inertia parameter, γ ,

$$v_0(\infty, T) \simeq -1 + \frac{d\phi'_p}{dT} - \gamma \frac{d^2 \phi'_p}{dT^2}. \quad (134)$$

Hence, the perturbed toroidal ion fluid velocity (divided by the magnitude of the unperturbed velocity) inside the island separatrix (where $v_0 = 0$) is

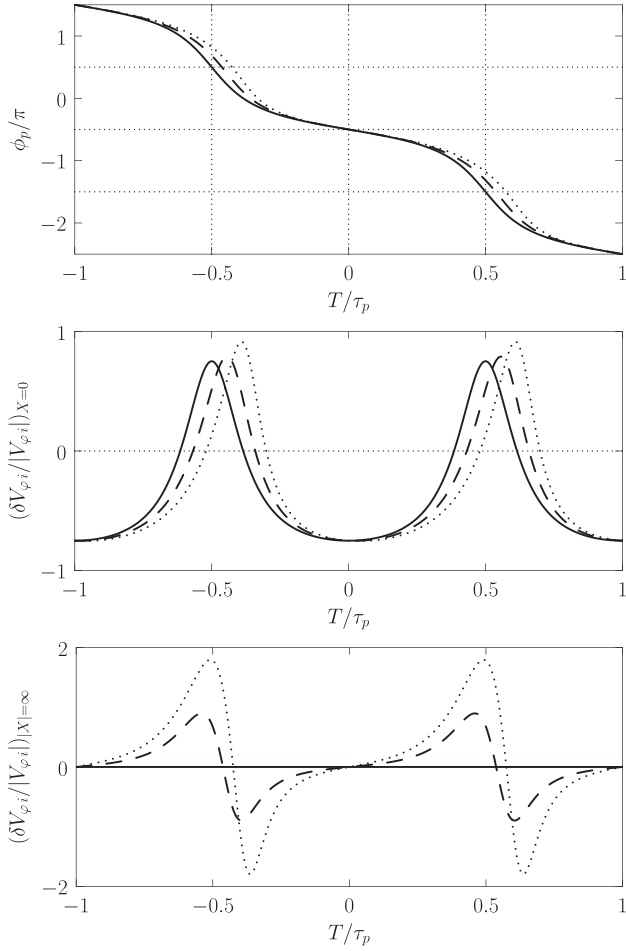


FIG. 3. Time evolution of a rotating pre-existing island chain interacting with a resonant error-field. The solid, dashed, and dotted curves are calculated with $\lambda_v = 0.75$ and $\gamma = 0.0, 1.0,$ and $2.0,$ respectively. The top, middle, and bottom panels show the island phase, the perturbed toroidal ion fluid velocity inside the separatrix, and the perturbed toroidal ion fluid velocity many island widths distant from the separatrix, respectively. The natural frequency is in the ion diamagnetic direction (i.e., $s_i = -1$). The calculation is made in the large perpendicular ion neoclassical flow damping limit, $\bar{\nu} \gg 1$, in which $\Gamma_1 = 0.18182\gamma$.

$$\begin{aligned} \left. \frac{\delta V_{\phi i}}{|V_{\phi i}|} \right|_{X=0} &= -s_i \left(-1 + \frac{d\phi'_p}{dT} \right) \\ &= s_i \left(\frac{\lambda_v \sin \phi'_p - \Gamma_1 \lambda_v \cos \phi'_p}{1 - \Gamma_1 \lambda_v \cos \phi'_p} \right), \end{aligned} \quad (135)$$

whereas that many island widths distant from the rational surface is

$$\left. \frac{\delta V_{\phi i}}{|V_{\phi i}|} \right|_{|X|=\infty} = -s_i \gamma \frac{d^2 \phi'_p}{dT^2} \simeq s_i \gamma \lambda_v \cos \phi'_p (1 - \lambda_v \sin \phi'_p). \quad (136)$$

Here, use has been made of Eqs. (129) and (130). Figures 2–4 also illustrate the typical time evolution of the perturbed toroidal ion fluid velocity associated with rotating solutions of the inviscid island phase evolution equation. It can be seen that the ion fluid velocity inside the island separatrix speeds up and slows down in tandem with the island rotation. Note, however, that finite ion inertia introduces a time lag

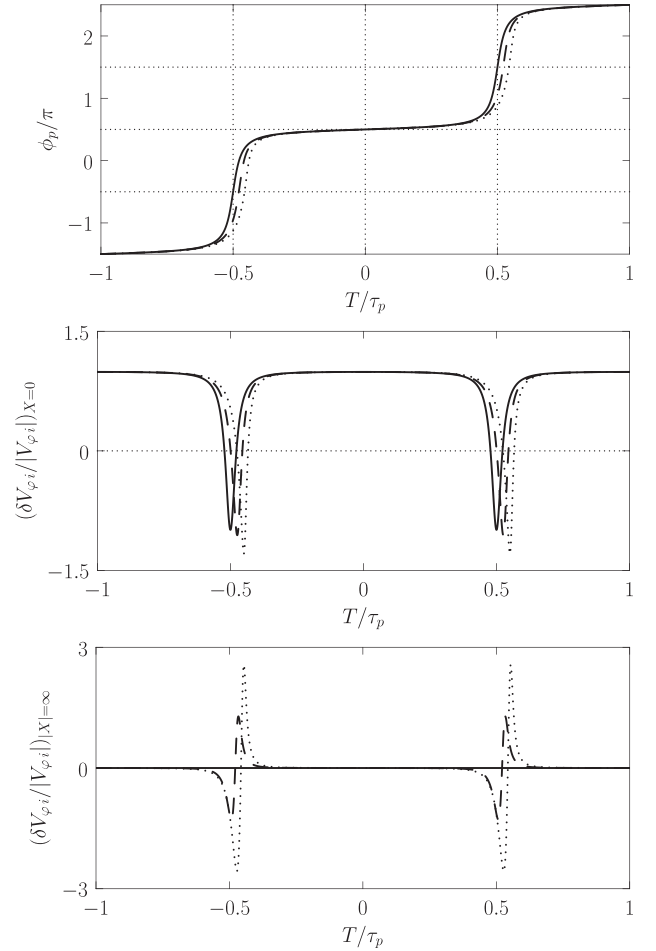


FIG. 4. Time evolution of a rotating pre-existing island chain interacting with a resonant error-field. The solid, dashed, and dotted curves are calculated with $\lambda_v = 0.99$ and $\gamma = 0.0, 1.0,$ and $2.0,$ respectively. The top, middle, and bottom panels show the island phase, the perturbed toroidal ion fluid velocity inside the separatrix, and the perturbed toroidal ion fluid velocity many island widths distant from the separatrix, respectively. The natural frequency is in the electron diamagnetic direction (i.e., $s_i = +1$). The calculation is made in the large perpendicular ion neoclassical flow damping limit, $\bar{\nu} \gg 1$, in which $\Gamma_1 = 0.18182\gamma$.

into the response of the ion fluid velocity to the acceleration of the island chain. It can also be seen that, in the absence of ion inertia (i.e., if $\gamma = 0$), there is no perturbation to the toroidal ion fluid velocity a long way from the island chain. On the other hand, in the presence of finite inertia, the perturbation a long way from the island chain is finite and roughly sinusoidal, but becomes increasing impulsive as the locking parameter, λ_v , approaches the critical magnitude unity (the same is true of the perturbation inside the separatrix).

G. Period-averaged solutions

Let us define a period-average operator

$$\begin{aligned} \langle \dots \rangle_T &= \frac{1}{\tau_p} \int_0^{\tau_p} (\dots) dT \\ &= \sqrt{1 - \lambda_v^2} \oint (\dots) \left(\frac{1 - \Gamma_1 \lambda_v \cos \phi'_p}{1 - \lambda_v \sin \phi'_p} \right) \frac{d\phi'_p}{2\pi} \end{aligned} \quad (137)$$

that averages over the rotation period of the island chain. It follows that²⁸

$$\left\langle \frac{d\phi'_p}{dT} \right\rangle_T = \sqrt{1 - \lambda_v^2}, \quad (138)$$

$$\left\langle \frac{d^2\phi'_p}{dT^2} \right\rangle_T = 0, \quad (139)$$

$$\begin{aligned} \langle \sin \phi'_p \rangle_T &= \frac{1 - \langle d\phi'_p/dT \rangle_T - \Gamma_1 \langle d^2\phi'_p/dT^2 \rangle_T}{\lambda_v} \\ &= \frac{1 - \sqrt{1 - \lambda_v^2}}{\lambda_v}, \end{aligned} \quad (140)$$

$$\langle \cos \phi'_p \rangle_T = -\frac{\Gamma_1}{\lambda_v} \sqrt{1 - \lambda_v^2} \left(1 - \sqrt{1 - \lambda_v^2} \right), \quad (141)$$

$$\left\langle \left(\frac{d\phi'_p}{dT} \right)^2 \right\rangle_T = \frac{\sqrt{1 - \lambda_v^2}}{\sqrt{1 - \Gamma_1^2 \lambda_v^2}} \approx \sqrt{1 - \lambda_v^2}. \quad (142)$$

If we define

$$f_s(\lambda_v) = \begin{cases} 1 - \sqrt{1 - \lambda_v^2} & \lambda_v \leq 1 \\ 1 & \lambda_v > 1, \end{cases} \quad (143)$$

and

$$f_c(\lambda_v) = \begin{cases} -\Gamma_1 \sqrt{1 - \lambda_v^2} \left(1 - \sqrt{1 - \lambda_v^2} \right) & \lambda_v \leq 1 \\ \sqrt{\lambda_v^2 - 1} & \lambda_v > 1, \end{cases} \quad (144)$$

then we can combine the previous results with the results of Sec. IV E to produce

$$\left\langle \frac{d\phi'_p}{dT} \right\rangle_T = 1 - f_s(\lambda_v), \quad (145)$$

$$\left\langle \frac{d^2\phi'_p}{dT^2} \right\rangle_T = 0, \quad (146)$$

$$\langle \sin \phi'_p \rangle_T = \frac{f_s(\lambda_v)}{\lambda_v}, \quad (147)$$

$$\langle \cos \phi'_p \rangle_T = \frac{f_c(\lambda_v)}{\lambda_v}, \quad (148)$$

$$\left\langle \left(\frac{d\phi'_p}{dT} \right)^2 \right\rangle_T = 1 - f_s(\lambda_v). \quad (149)$$

Equations (145)–(149) are now valid for both rotating and locked solutions.

It follows from Eqs. (135), (136), (145), and (146) that

$$\left\langle \frac{\delta V_{\phi i}}{|V_{\phi i}|} \Big|_{X=0} \right\rangle_T = -s_i \left(-1 + \left\langle \frac{d\phi'_p}{dT} \right\rangle_T \right) = s_i f_s(\lambda_v), \quad (150)$$

$$\left\langle \frac{\delta V_{\phi i}}{|V_{\phi i}|} \Big|_{|X|=\infty} \right\rangle_T = -s_i \gamma \left\langle \frac{d^2\phi'_p}{dT^2} \right\rangle_T = 0. \quad (151)$$

In other words, there is a finite period-averaged shift (relative to the error-field-free state) in the toroidal ion fluid velocity inside the separatrix of a locked magnetic island chain, whereas the period-averaged shift many island widths distant from the separatrix is zero. The latter result follows because the period-averaged shift is localized in the immediate vicinity of the island chain due to the action of perpendicular ion flow damping.²⁹

To the first order in γ , Eq. (101) yields

$$\begin{aligned} v_0(\Omega, T) &= -\frac{1}{(1 + \bar{\nu}) \langle 1 \rangle \langle X^2 \rangle f} \\ &\times \left[\bar{\nu} \left(1 - \frac{d\phi'_p}{dT} \right) - \gamma \left(1 - \frac{\bar{\nu}}{f} \right) \frac{d^2\phi'_p}{dT^2} \right]. \end{aligned} \quad (152)$$

Thus, it follows from Eq. (83) that

$$m(\Omega, T) = \frac{\bar{\nu}}{1 + \bar{\nu}} \frac{1 - d\phi'_p/dT}{\langle X^2 \rangle f} - \frac{\gamma}{1 + \bar{\nu}} \frac{\langle 1 \rangle \langle X^2 \rangle - 1}{\langle 1 \rangle \langle X^2 \rangle^2 f^2} \frac{d^2\phi'_p}{dT^2}, \quad (153)$$

and

$$v_0 + \frac{m}{\langle 1 \rangle} = -\frac{\bar{\nu}}{1 + \bar{\nu}} \frac{\gamma}{\langle 1 \rangle \langle X^2 \rangle f} \frac{d^2\phi'_p}{dT^2}. \quad (154)$$

Hence, making use of Eqs. (145)–(149), we deduce that

$$\langle v_0 + \frac{m}{\langle 1 \rangle} \rangle_T = 0, \quad (155)$$

$$\langle m \rangle_T = \frac{\bar{\nu}}{1 + \bar{\nu}} \frac{f_s(\lambda_v)}{\langle X^2 \rangle f}, \quad (156)$$

$$\langle m^2 \rangle_T = \left(\frac{\bar{\nu}}{1 + \bar{\nu}} \right)^2 \frac{f_s(\lambda_v)}{\langle X^2 \rangle^2 f^2}. \quad (157)$$

H. Determination of period-averaged island width

Given that the island chain's width is assumed to evolve on a much longer timescale than its phase, it makes sense to average the island width evolution equation, (59), over the rotation period of the island chain to give

$$\begin{aligned} 0 &= \Delta' r_s + \beta \frac{r_s}{w} \left[I_v \hat{\nu}_{\theta i} |v_{\perp i} - v_{\theta i}| \lambda_v \langle \cos \phi_p \rangle_T \right. \\ &\quad \left. + \alpha_n \left(\frac{\epsilon \nu_{\theta e} \tau_e}{1 + \epsilon \nu_{\theta e} \tau_e} \right) \langle I_{b0} \rangle_T + \epsilon \langle I_p \rangle_T - \alpha_c (1 + \tau) \langle I_g \rangle_T \right], \end{aligned} \quad (158)$$

where

$$\langle I_{b0} \rangle_T = \int_1^\infty 4 \left[\frac{v_{\theta i} + \tau v_{\theta e}}{\langle 1 \rangle \langle X^2 \rangle} + (v_{\perp i} - v_{\theta i}) \langle v_0 + \frac{m}{\langle 1 \rangle} \rangle_T \right] \langle \cos \zeta \rangle d\Omega, \quad (159)$$

$$\begin{aligned} \langle I_p \rangle_T = \int_{1-}^{\infty} \partial\Omega \left[\frac{(v_{\theta i} - 1) v_{\theta i}}{\langle X^2 \rangle} + (2v_{\theta i} - 1)(v_{\perp i} - v_{\theta i}) \frac{\langle m \rangle_T}{\langle X^2 \rangle} \right. \\ \left. + (v_{\perp i} - v_{\theta i})^2 \langle m^2 \rangle_T \right] \langle \tilde{X}^2 \tilde{X}^2 \rangle d\Omega, \end{aligned} \quad (160)$$

$$\langle I_g \rangle_T = \int_1^{\infty} 2 \frac{\langle |\tilde{X}| \tilde{X}^2 \rangle}{\langle X^2 \rangle} d\Omega. \quad (161)$$

Here, use has been made of Eqs. (61)–(63), (73), (80), (81), (87), (88), and (103). Thus, it follows from Eqs. (148) and (155)–(157) that

$$\begin{aligned} 0 = \Delta' r_s + \beta \frac{r_s}{w} \left[I_v \hat{v}_{\theta i} |v_{\perp i} - v_{\theta i}| f_c(\lambda_v) \right. \\ \left. + I_b \alpha_n \left(\frac{\epsilon \nu_{\theta e} \tau_e}{1 + \epsilon \nu_{\theta e} \tau_e} \right) (v_{\theta i} + \tau v_{\theta e}) + I_{p0} \epsilon (v_{\theta i} - 1) v_{\theta i} \right. \\ \left. + I_{p1} \epsilon (2v_{\theta i} - 1)(v_{\perp i} - v_{\theta i}) f_s(\lambda_v) + I_{p2} \epsilon (v_{\perp i} - v_{\theta i})^2 f_s(\lambda_v) \right. \\ \left. - I_b \alpha_c (1 + \tau) \right], \end{aligned} \quad (162)$$

where¹⁹

$$I_b = \int_1^{\infty} 16 \left(\frac{\mathcal{D}}{\mathcal{C}} - \frac{1}{\mathcal{A}} \right) k^2 dk = 1.58, \quad (163)$$

$$I_{p0} = \frac{2\pi}{3} - \int_{1+}^{\infty} \frac{4}{\mathcal{C}} \left(\frac{\mathcal{E} \mathcal{A}}{\mathcal{C}^2} - 1 \right) dk = 1.38, \quad (164)$$

$$\begin{aligned} I_{p1} = \frac{2\pi}{3} \left(\frac{\bar{\nu}}{1 + \bar{\nu}} \right) - \int_{1+}^{\infty} \frac{4Y}{\mathcal{C}} \left(\frac{\mathcal{E} \mathcal{A}}{\mathcal{C}^2} - 1 \right) dk \\ + \int_{1+}^{\infty} 2 dk Y \left(\frac{\mathcal{E}}{\mathcal{C}^2} - \frac{1}{\mathcal{A}} \right) k dk, \end{aligned} \quad (165)$$

$$\begin{aligned} I_{p2} = \frac{2\pi}{3} \left(\frac{\bar{\nu}}{1 + \bar{\nu}} \right)^2 - \int_{1+}^{\infty} \frac{4Y^2}{\mathcal{C}} \left(\frac{\mathcal{E} \mathcal{A}}{\mathcal{C}^2} - 1 \right) dk \\ + \int_{1+}^{\infty} 4Y dk Y \left(\frac{\mathcal{E}}{\mathcal{C}^2} - \frac{1}{\mathcal{A}} \right) k dk, \end{aligned} \quad (166)$$

and

$$Y(k) = \frac{\bar{\nu}}{(1 + \bar{\nu})f(k)}. \quad (167)$$

Here, the functions $\mathcal{A}(k)$, $\mathcal{C}(k)$, $\mathcal{D}(k)$, and $\mathcal{E}(k)$ are defined in the Appendix. It is relatively straightforward to demonstrate that $I_{p1} = I_{p2} = I_{p0}$ in the large perpendicular ion neoclassical flow damping limit, $\bar{\nu} \gg 1$, whereas $I_{p1} = I_{p2} = 0$ in the opposite limit, $\bar{\nu} \ll 1$. Note that, for the sake of simplicity, we are neglecting the modification of the ion polarization term in the island width evolution equation due to the finite width of the separatrix boundary layer.¹⁹

Obviously, Eq. (162) can be solved to determine the period-averaged island width, w (recalling that β , λ_v , α_n , and α_c are functions of w). For the sake of consistency, the solution must be such that $w/r_s \gg m_{\theta}/(k_{\theta} V_{*i} |v_{\perp i} - v_{\theta i}| \tau_R)$.

The first term within the square brackets in Eq. (162) represents the stabilizing/destabilizing effect of the error-

field, the second term represents the destabilizing effect of the perturbed bootstrap current, the third, fourth, and fifth terms represent the stabilizing/destabilizing effect of the perturbed ion polarization current, and the final term represents the stabilizing effect of the magnetic field-line curvature.

Ion inertia only affects the error-field term in Eq. (162). In fact, ion inertia causes a rotating island chain to spend slightly more time in a stabilizing phase relation with respect to the error-field than in a destabilizing phase relation (see Sec. IV F). It follows that, in the presence of ion inertia, the error-field has a net stabilizing effect on the island chain, as long the chain is rotating.²² Of course, the island chain always locks to the error-field in a destabilizing phase relation (see Sec. IV E). Hence, a rotating island chain is stabilized by a resonant error-field, whereas a locked island chain is destabilized. It can be seen, from Eq. (144), first, that the stabilizing effect of the error-field approaches zero as the locking parameter, λ_v , approaches zero; second, that the stabilizing effect also approaches zero as the locking parameter approaches the critical value unity; and, finally, that the stabilizing effect attains its maximum value when $\lambda_v = \sqrt{3}/2$.

Note that the bootstrap and curvature terms in Eq. (162) are both independent of the island locking parameter (i.e., they are the same for rotating and locked island chains). On the other hand, in the large perpendicular ion neoclassical flow damping limit, $\bar{\nu} \gg 1$, the ion polarization term is different for rotating and locked island chains. In particular, the polarization term takes the form $\beta (r_s/w) I_{p0} \epsilon (v_{\theta i} - 1) v_{\theta i}$ for a freely rotating island chain (i.e., $\lambda_v = 0$), and takes the form $\beta (r_s/w) I_{p0} \epsilon (v_{\perp i} - 1) v_{\perp i}$ for a locked island chain.¹⁹ The former form is usually stabilizing (i.e., negative), whereas the latter can be destabilizing (especially in the presence of a strong external toroidal momentum source).¹⁹

V. ERROR-FIELD-MAINTAINED MAGNETIC ISLAND CHAIN

A. Introduction

Suppose that the plasma equilibrium is tearing stable (i.e., $\Delta' < 0$), which implies that the magnetic island chain is maintained in the plasma by the action of the resonant error-field (i.e., there would be no island chain in the absence of the error-field). In this case, the island width is forced to evolve on the same timescale as the island phase.^{30–32} In order to investigate this problem, we shall adopt a simplified model in which the bootstrap, ion polarization, and magnetic field-line curvature terms are neglected in the island width evolution equation, ion viscosity is neglected in the island phase evolution equation, and all terms in the inviscid island phase evolution equation that are quadratic (or higher order) in the ion inertia parameter, γ , are also neglected. Furthermore, we shall assume that the analysis of Sec. IV B remains valid (which implies that the island width evolves on a timescale that is much longer than that required for density to diffuse across the inner region). It follows from Eqs. (59) and (127) that

$$I_i \tau_R \frac{d}{dt} \left(\frac{w}{r_s} \right) = -(-\Delta' r_s) + 2 m_\theta \left(\frac{w_v}{w} \right)^2 \cos \phi'_p \quad (168)$$

and

$$\Gamma_1 \frac{d^2 \phi'_p}{dT^2} + \frac{d\phi'_p}{dT} + \lambda_v \sin \phi'_p = 1, \quad (169)$$

where $T = |v_{\perp i} - v_{\theta i}| k_\theta V_{*i} t$, $\phi'_p = \text{sgn}(v_{\perp i} - v_{\theta i}) \phi_p$, $\lambda_v = 2 m_\theta w_v^2 / (I_v \beta |v_{\perp i} - v_{\theta i}| \hat{v}_{\theta i} r_s w)$, $\beta = \beta_i (q_s / \epsilon_s)^2 (L_q / L_n)^2 \times (\rho_{\theta i} / w)^2$, and

$$I_i = \int_0^\infty \frac{64 [(k^2 - 1/2) \mathcal{A} - k^2 \mathcal{C}]^2}{\mathcal{A}} dk = 3.2908. \quad (170)$$

Here, $\mathcal{A}(k)$ and $\mathcal{C}(k)$ are defined in the [Appendix](#). Equations (168) and (169) can be rewritten in the form

$$\frac{1}{\epsilon_R} \frac{d}{dT} \left[\left(\frac{w}{w_v} \right)^3 \right] = - \left(\frac{w}{w_v} \right)^2 + \cos \phi'_p, \quad (171)$$

$$\Gamma_1 \frac{d^2 \phi'_p}{dT^2} + \frac{d\phi'_p}{dT} + \delta_v \left(\frac{w}{w_v} \right) \sin \phi'_p = 1, \quad (172)$$

where

$$\epsilon_R = \frac{6 m_\theta r_s}{I_i k_\theta V_{*i} |v_{\perp i} - v_{\theta i}| \tau_R w_v}, \quad (173)$$

$$\delta_v = \frac{2 m_\theta w_v}{I_v \beta_v |v_{\perp i} - v_{\theta i}| \hat{v}_{\theta i} r_s}, \quad (174)$$

and $\beta_v = \beta_i (q_s / \epsilon_s)^2 (L_q / L_n)^2 (\rho_{\theta i} / w_v)^2$. Here, for the sake of simplicity, we have assumed that $\Delta' r_s = -2 m_\theta$, which is generally the case when $m_\theta \gg 1$. (This assumption is particularly appropriate to experiments in which RMPs are used to suppress ELMs.) Incidentally, we expect that $\epsilon_R \ll 1$, given the fact that the resistive evolution timescale, τ_R , is usually much longer than any other relevant timescale in a high temperature tokamak plasma.

B. Locked solutions

Let us search for locked solutions of Eqs. (171) and (172), in which ϕ'_p is independent of time. Equation (171) yields

$$\frac{w}{w_v} = \cos^{1/2} \phi'_p, \quad (175)$$

which can only be satisfied provided that $-\pi/2 \leq \phi'_p \leq \pi/2$. Equation (172) then reduces to

$$\Gamma_1 \frac{d^2 \phi'_p}{dT^2} + \frac{d\phi'_p}{dT} + F(\phi'_p) = 0, \quad (176)$$

where

$$F(\phi'_p) = \delta_v \cos^{1/2} \phi'_p \sin \phi'_p - 1. \quad (177)$$

If $\phi'_p = \phi'_{p(0)}$ is an equilibrium solution of Eq. (176), then

$$F(\phi'_{p(0)}) = 0. \quad (178)$$

Moreover, writing $\phi'_p(T) = \phi'_{p(0)} + \delta\phi_p(T)$, we arrive at

$$\Gamma_1 \frac{d^2 \delta\phi'_p}{dT^2} + \frac{d\delta\phi'_p}{dT} + F'(\phi'_{p(0)}) \delta\phi'_p = 0, \quad (179)$$

where $F' = dF/d\phi_p$. However, the previous equation is simply a damped harmonic oscillator equation, which is known to have stable equilibria when

$$F'(\phi'_{p(0)}) > 0. \quad (180)$$

Hence, the stable solutions of Eq. (178) are such that $\delta_v > \delta_{v \text{ unlock}}$ and $0 \leq \phi'_p < \sin^{-1}(\sqrt{2/3})$, where

$$\delta_{v \text{ unlock}} = \left(\frac{\sqrt{27}}{2} \right)^{1/2}. \quad (181)$$

It follows that stable locked solutions are only possible when the so-called *unlocking parameter*, δ_v , exceeds the critical value $\delta_{v \text{ unlock}}$. Moreover, the solutions are all such that $\cos \phi_p = \cos \phi'_p > 0$: i.e., such that the island chain locks in a destabilizing phase relation with respect to the error-field. Incidentally, it is valid to neglect the time dependence of the island width when assessing the stability of locked solutions because we are assuming that $\epsilon_R \ll 1$ [see Eq. (171)].

C. Rotating solutions

Let us search for rotating solutions of Eqs. (171) and (172) in which ϕ'_p varies in time. Writing

$$\xi = \frac{1}{\epsilon_R} \left(\frac{w}{w_v} \right)^3. \quad (182)$$

Equations (171) and (172) yield

$$\frac{d\xi}{dT} = -\epsilon_R^{2/3} \xi^{2/3} + \cos \phi'_p, \quad (183)$$

$$\Gamma_1 \frac{d^2 \phi'_p}{dT^2} + \frac{d\phi'_p}{dT} + \zeta_v \xi^{1/3} \sin \phi'_p = 1, \quad (184)$$

where

$$\zeta_v = \epsilon_R^{1/3} \delta_v. \quad (185)$$

Note that we expect $\xi \sim \mathcal{O}(1)$ for rotating solutions. It follows that rotating solutions are characterized by much smaller (by a factor $1/\epsilon_R^{1/3}$) island widths than locked solutions. Hence, for rotating solutions, the so-called *shielding factor* (i.e., the factor by which the reconnected flux at the rational surface is reduced relative to the locked solution) is of order $1/\epsilon_R^{2/3}$.

Given that $\epsilon_R \ll 1$ and $\xi \sim \mathcal{O}(1)$, Eq. (183) reduces to

$$\frac{d\xi}{dT} = \cos \phi'_p. \quad (186)$$

Now, to the lowest order in ζ_v and Γ_1 , Eq. (184) gives

$$\frac{d\phi'_p}{dT} \simeq 1. \quad (187)$$

The previous two equations imply that

$$\xi \simeq \sin \phi'_p. \quad (188)$$

Thus, to the next order in ζ_v and Γ_1 , we have

$$\frac{d\phi'_p}{dT} = 1 - \zeta_v \sin^{4/3} \phi'_p, \quad (189)$$

$$\frac{d^2\phi'_p}{dT^2} = -\frac{4}{3} \zeta_v \sin^{1/3} \phi'_p \cos \phi'_p \frac{d\phi'_p}{dT}, \quad (190)$$

which can be combined to give

$$\frac{d\phi'_p}{dT} = \frac{1 - \zeta_v \sin^{4/3} \phi'_p}{1 - (4/3) \Gamma_1 \zeta_v \sin^{1/3} \phi'_p \cos \phi'_p}. \quad (191)$$

We also have

$$\frac{d\xi}{d\phi'_p} = \frac{d\xi}{dT} \frac{dT}{d\phi'_p} = \left[\frac{1 - (4/3) \Gamma_1 \zeta_v \sin^{1/3} \phi'_p \cos \phi'_p}{1 - \zeta_v \sin^{4/3} \phi'_p} \right] \cos \phi'_p. \quad (192)$$

Thus, we can write

$$\xi(\phi'_p) = \int_{\phi'_{p0}}^{\phi'_p} \left[\frac{1 - (4/3) \Gamma_1 \zeta_v \sin^{1/3} y \cos y}{1 - \zeta_v \sin^{4/3} y} \right] \cos y dy. \quad (193)$$

Here, ϕ'_{p0} is chosen such that $\xi(\phi'_{p0} + \pi) = 0$. In other words, the rotating island chain is born at zero width with the helical phase ϕ'_{p0} . However, the plasma rotation forces the island phase, ϕ'_p , to continually increase in time [see Eq. (189)]. This phase increase initially moves the chain into a destabilizing phase relation with the error-field, causing its width to increase in time. Eventually, however, the rotation forces the chain into a stabilizing phase relation with the error-field, and its width consequently decreases. The width reaches zero again when the helical phase attains the value $\xi(\phi'_{p0} + \pi) = 0$, at which point the phase jumps discontinuously to $2\pi + \phi'_{p0}$, and the process repeats itself *ad infinitum*. The discontinuous jump in helical phase of π radians is associated with the conversion of the island O-points into X-points, and vice versa (i.e., with a reversal in the sign of the reconnected magnetic flux at the rational surface).³² Figure 5 shows the birth phase, ϕ'_{p0} , plotted as a function of the locking parameter, ζ_v , for various values of the ion inertia parameter, γ . It can be seen that the birth phase is always close to zero, and is a weakly decreasing function of γ .

The normalized rotation period of the island chain is

$$\tau_p = \int_{\phi'_{p0}}^{\phi'_{p0} + \pi} \left[\frac{1 - (4/3) \Gamma_1 \zeta_v \sin^{1/3} y \cos y}{1 - \zeta_v \sin^{4/3} y} \right] dy. \quad (194)$$

Figure 6 shows τ_p plotted as a function of the so-called *locking parameter*, ζ_v . The rotation period is found to have

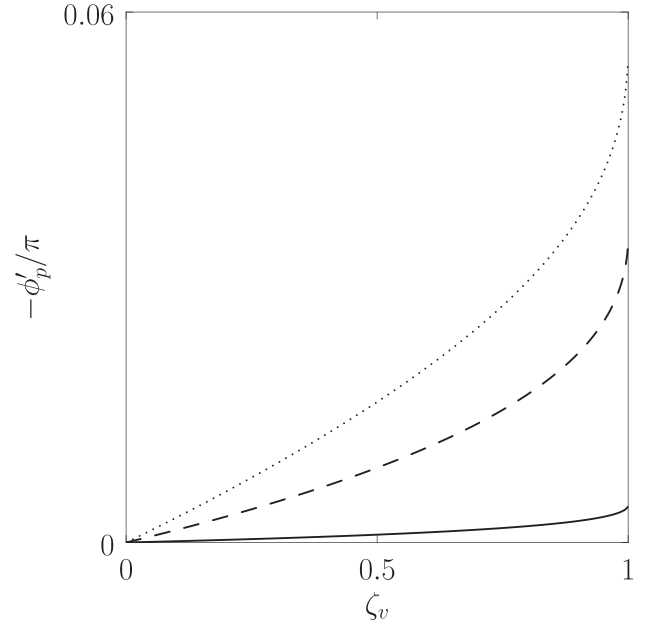


FIG. 5. The birth phase, ϕ'_{p0} , of a rotating error-field-maintained magnetic island chain as a function of the locking parameter, ζ_v . The solid, dashed, and dotted curves correspond to $\gamma = 0.1$, $\gamma = 1.0$, and $\gamma = 2.0$, respectively. The calculation is made in the large perpendicular ion neoclassical flow damping limit, $\bar{\nu} \gg 1$, in which $\Gamma_1 = 0.18182\gamma$.

no dependence on γ . Moreover, the period goes to infinity as the locking parameter approaches the critical value unity; this indicates a transition to locked solutions when ζ_v exceeds the critical value unity. Note that $\zeta_v \propto |\omega_0|^{-4/3}$, where ω_0 is the natural frequency defined in Eq. (74). It follows that locked solutions are more likely to form when the natural frequency is relatively small.

Referring to Eqs. (175), (181), (182), (185), and (188), it is clear that locked solutions of the inviscid island phase

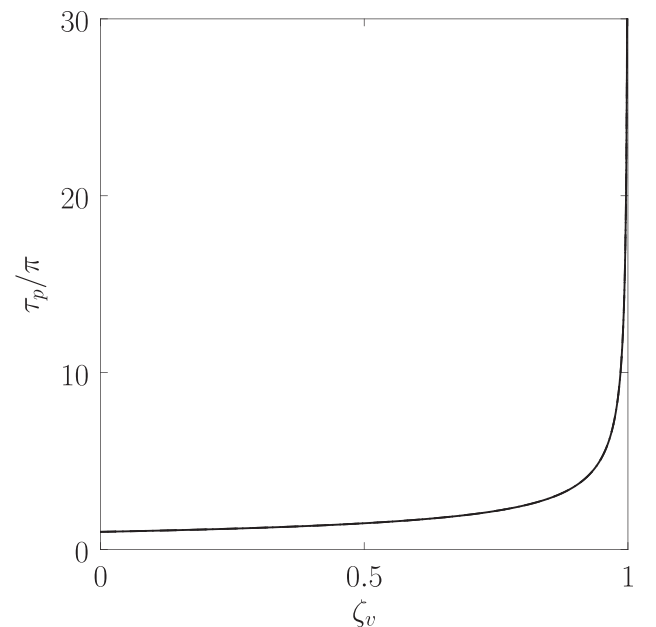


FIG. 6. The normalized rotation period, τ_p , of an error-field-maintained magnetic island chain as a function of the locking parameter, ζ_v . The rotation period is found to be independent of γ .

evolution equation are characterized by $w/w_v \sim \mathcal{O}(1)$, whereas rotating solutions are characterized by $w/w_v \sim \mathcal{O}(\epsilon_R^{1/3}) \ll 1$. Moreover, a locked solution is converted into an unlocked solution when the unlocking parameter, δ_v , falls below the critical value $(\sqrt{27}/2)^{1/2}$. On the other hand, a rotating solution is converted into a locked solution when δ_v exceeds the critical value $1/\epsilon_R^{1/3}$. Given that $1/\epsilon_R^{1/3} \gg (\sqrt{27}/2)^{1/2}$, we deduce that, for the case of an error-field-maintained island chain, there is considerable hysteresis in the locking/unlocking process. In other words, once an error-field has exceeded the critical magnitude required to produce a locked island chain, the magnitude of the error-field must be reduced by a large factor before the locked chain starts to rotate again (and its width is, consequently, considerably reduced).³⁰ This behavior is in marked contrast to that discussed in Sec. IV, where, for the case of a pre-existing island chain, the locked and unlocked solutions have approximately the same width, and there is no hysteresis in the locking/unlocking process.

Equation (191) can be integrated to give

$$T(\phi'_p) = -\frac{1}{2} + \int_{\phi'_{p0}}^{\phi'_p} \left[\frac{1 - (4/3) \Gamma_1 \zeta_v \sin^{1/3} y \cos y}{1 - \zeta_v \sin^{4/3} y} \right] dy, \quad (195)$$

assuming that $\phi'_p = \phi'_{p0}$ when $T = -1/2$. Moreover, making use of Eqs. (133), (134), (190), and (191), the perturbed toroidal ion fluid velocity (divided by the magnitude of the unperturbed velocity) inside the island separatrix is

$$\left. \frac{\delta V_{\phi i}}{|V_{\phi i}|} \right|_{X=0} = s_i \left[\frac{\zeta_v \sin^{4/3} \phi'_p - (4/3) \Gamma_1 \zeta_v \sin^{1/3} \phi'_p \cos \phi'_p}{1 - (4/3) \Gamma_1 \zeta_v \sin^{1/3} \phi'_p \cos \phi'_p} \right], \quad (196)$$

whereas that many island widths distant from the rational surface is

$$\left. \frac{\delta V_{\phi i}}{|V_{\phi i}|} \right|_{|X|=\infty} = s_i \frac{4}{3} \gamma \zeta_v \sin^{1/3} \phi'_p \cos \phi'_p (1 - \zeta_v \sin^{4/3} \phi'_p). \quad (197)$$

Figures 7–9 illustrate the typical time evolution of the island phase, the normalized island width $\xi^{1/3} = w/(\epsilon_R^{1/3} w_v)$, and the perturbed toroidal ion fluid velocity, associated with rotating solutions of the inviscid island phase evolution equation. It can be seen that the phase evolution of a rotating error-field-maintained magnetic island chain is similar to that of a pre-existing island chain (see Figs. 2–4), except for the presence of discontinuous phase jumps in the former case. These jumps are necessitated by the fact that an error-field-maintained island chain cannot exist in a phase relationship with the error-field that is such that $\sin \phi'_p < 0$ [see Eq. (188)]. The jumps can only occur when the island width falls instantaneously to zero, and are such that the island's helical phase advances by $s_i \pi$ radians (i.e., the island O-points are converted into X-points, and vice versa).³² It can also be seen that the time evolution of the perturbed toroidal ion fluid velocity associated a rotating error-field-maintained magnetic island

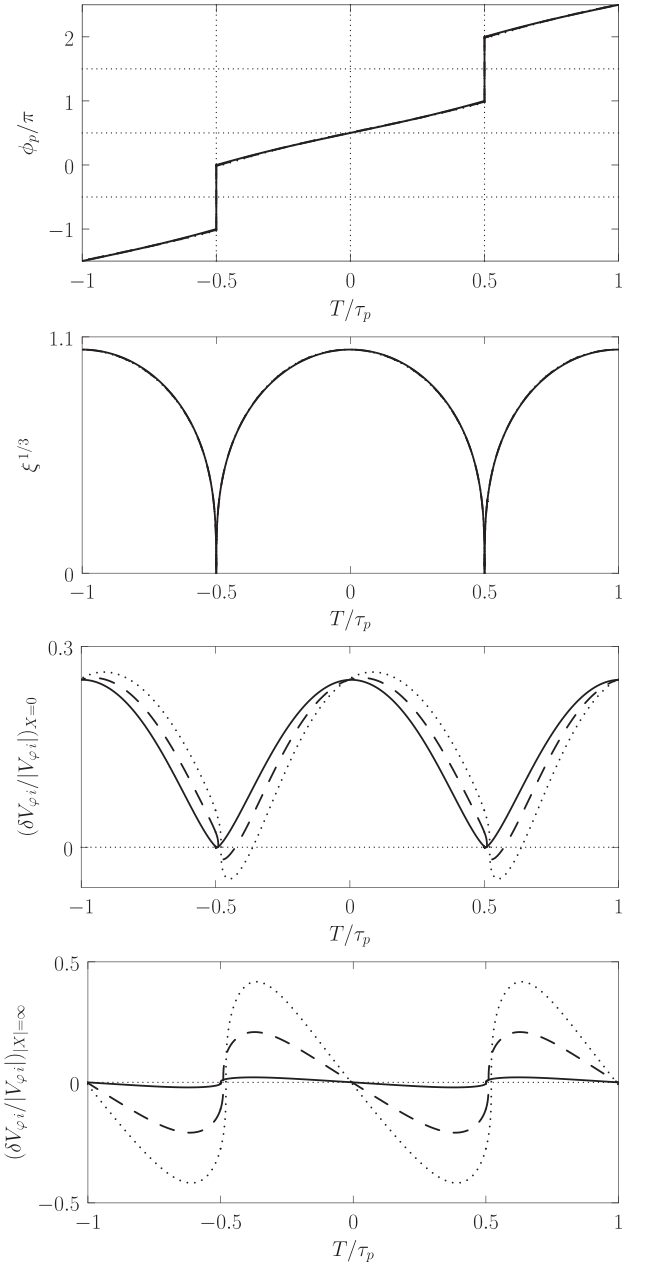


FIG. 7. Time evolution of a rotating error-field-maintained magnetic island chain. The solid, dashed, and dotted curves are calculated with $\zeta_v = 0.25$ and $\gamma = 0.1, 1.0,$ and 2.0 , respectively. The, first (from the top), second, third, and fourth panels show the island phase, the normalized island width, the perturbed toroidal ion fluid velocity inside the separatrix, and the perturbed toroidal ion fluid velocity many island widths distant from the separatrix, respectively. The natural frequency is in the electron diamagnetic direction (i.e., $s_i = +1$). The calculation is made in the large perpendicular ion neoclassical flow damping limit, $\bar{\nu} \gg 1$, in which $\Gamma_1 = 0.18182 \gamma$.

chain interacting with a resonant error-field is fairly similar to that of a pre-existing island chain (see Figs. 2–4). The main difference is that, in the former case, the fluid velocity inside the separatrix only shifts in the direction associated with island deceleration. As before, finite ion inertia introduces a time lag into the response of the ion fluid velocity to the acceleration of the island chain, and also gives rise to a finite perturbation (whose average over the rotation period of the island is zero) of the toroidal ion fluid velocity many island widths distant from the island separatrix.

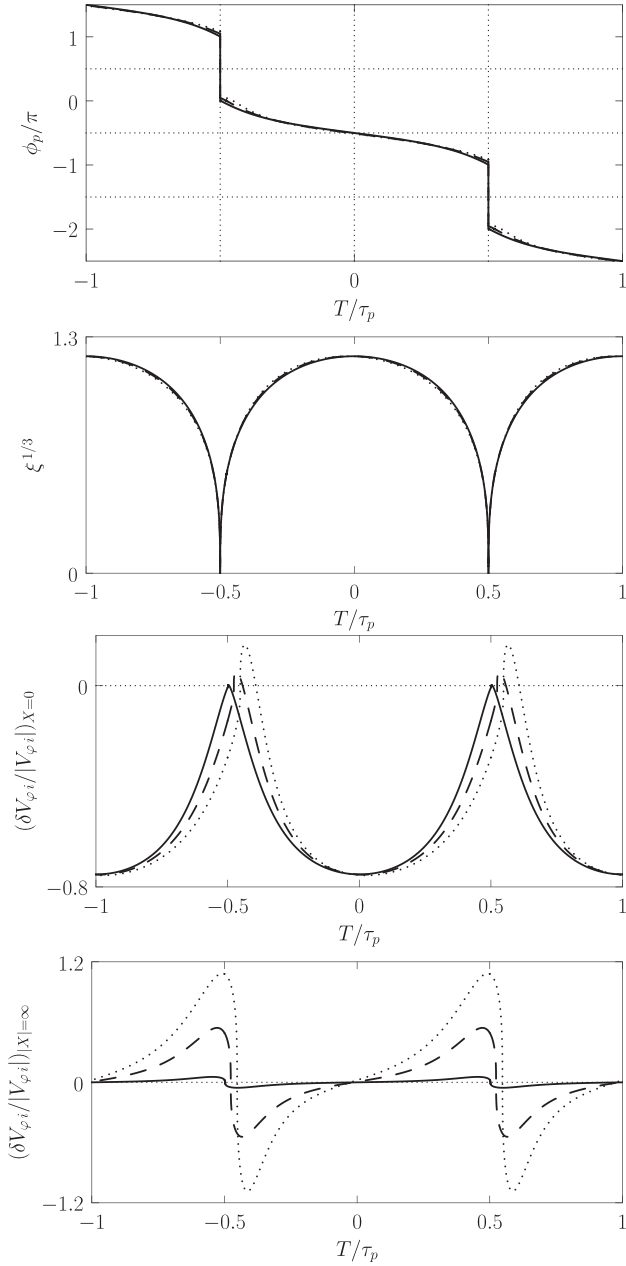


FIG. 8. Time evolution of a rotating error-field-maintained magnetic island chain. The solid, dashed, and dotted curves are calculated with $\zeta_v = 0.75$ and $\gamma = 0.1, 1.0,$ and $2.0,$ respectively. The, first (from the top), second, third, and fourth panels show the island phase, the normalized island width, the perturbed toroidal ion fluid velocity inside the separatrix, and the perturbed toroidal ion fluid velocity many island widths distant from the separatrix, respectively. The natural frequency is in the ion diamagnetic direction (i.e., $s_i = -1$). The calculation is made in the large perpendicular ion neoclassical flow damping limit, $\bar{\nu} \gg 1$, in which $\Gamma_1 = 0.18182 \gamma$.

VI. SUMMARY AND DISCUSSION

This paper investigates the interaction of a single-helicity magnetic island chain with a resonant error-field in a quasi-cylindrical, low- β , tokamak plasma. In particular, the nonlinear, neoclassical, two-fluid treatment of the problem presented in Ref. 19 is generalized to allow for explicit time dependence. Aside from the ability to more accurately treat time-varying problems, the main physical effect that is introduced into the model by the incorporation of explicit time dependence is *ion inertia*.

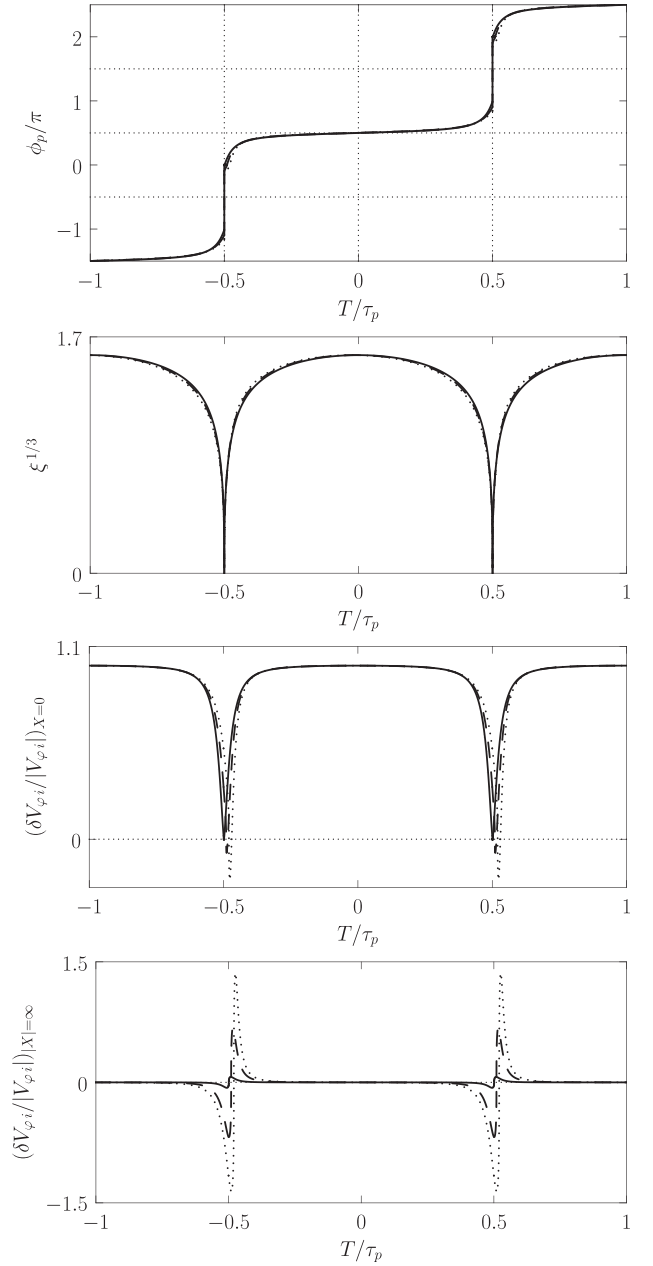


FIG. 9. Time evolution of a rotating error-field-maintained magnetic island chain. The solid, dashed, and dotted curves are calculated with $\zeta_v = 0.99$ and $\gamma = 0.1, 1.0,$ and $2.0,$ respectively. The, first (from the top), second, third, and fourth panels show the island phase, the normalized island width, the perturbed toroidal ion fluid velocity inside the separatrix, and the perturbed toroidal ion fluid velocity many island widths distant from the separatrix, respectively. The natural frequency is in the ion diamagnetic direction (i.e., $s_i = -1$). The calculation is made in the large perpendicular ion neoclassical flow damping limit, $\bar{\nu} \gg 1$, in which $\Gamma_1 = 0.18182 \gamma$.

The incorporation of explicit time dependence [i.e., including the $\partial/\partial t$ terms on the left-hand sides of the governing nonlinear, neoclassical, and two-fluid equations, (1)–(4)] necessitates a slight modification of the spatial boundary conditions, (7)–(10). To be more exact, in this paper, the spatial gradients of the density, scalar potential, and parallel ion velocity, rather than the actual values of these quantities, are fixed a long way from the island chain. Furthermore, when determining the flow profiles in the vicinity of a time-dependent island chain, it is found to be more convenient to

express all quantities in terms of the parallel ion velocity, rather than the ion stream function (as was our previous practice).

After considerable analysis, we are able to derive a closed set of equations, (97)–(99), that govern the phase evolution of a magnetic island chain interacting with a resonant error-field. One of these equations, (97), is a time-dependent, second-order, partial differential equation for the perturbed parallel ion velocity profile outside the island separatrix; this equation must be solved subject to a pair of straightforward spatial boundary conditions, (98). The final equation, (99), is an integral equation, involving the parallel ion velocity profile that implicitly determines the island phase.

In the limit in which ion viscosity can be neglected with respect to ion neoclassical flow damping, the previously mentioned closed set of equations can be reduced to a single, infinite-order, ordinary differential equation, (102), that explicitly determines the evolution of the island phase. Finally, in the limit when ion inertia is relatively small, the previously mentioned infinite-order, ordinary differential equation simplifies to give a second-order, ordinary differential equation, (127) that has the same mathematical form as the equation of motion of a simple pendulum subject to a constant torque. Most of the analysis presented in this paper is performed using this simplified phase evolution equation.

In Sec. IV, we investigate the interaction of a pre-existing island chain with a resonant error-field. In this case, it is reasonable to assume that the island width evolves on a much longer timescale than the island phase (given that the resistive timescale is usually much longer than any other relevant timescale in the problem). We find that there are two types of solution. First, *locked solutions* in which the island phase relative to the error-field is constant (which implies that the island chain is stationary in the laboratory frame). Second, *rotating solutions* in which the island phase increases (or decreases) continually in time. One novel feature of our analysis is the existence of an exact analytic form, (132), for rotating solutions of the phase evolution equation. Only rotating solutions exist when the so-called locking parameter, λ_v [see Eq. (103)], lies below the critical value unity, whereas only locked solutions exist when λ_v exceeds unity. The (stable) locked solutions are all such that the island chain is destabilized by the error-field. As the locking parameter approaches the critical value unity, the island rotation becomes increasingly uneven, under the action of the electromagnetic torque exerted by the error-field. However, in the absence of ion inertia, the island chain spends as much time having a stabilizing phase relation with respect to the error-field as it does having a destabilizing phase relation. On the other hand, in the presence of ion inertia, the island chain spends slightly more time having a stabilizing phase relation with respect to the error-field than it does having a destabilizing phase relation. The net result is that a rotating island chain is stabilized via interaction with a resonant error-field, whereas a locked island chain is destabilized.

Ion inertia introduces a time lag into the response of the toroidal ion fluid velocity in the vicinity of the magnetic island chain to the chain's acceleration. Ion inertia also gives

rise to a transient response of the toroidal ion fluid velocity many island widths distant from the separatrix to the island acceleration. (In the absence of ion inertia, this response is zero, due to the action of perpendicular neoclassical ion flow damping.)

The mean island width is determined by averaging the island width evolution equation over the rotation period of the island chain. Locked and rotating solutions have similar widths. The terms in the island width evolution equation due to the perturbed bootstrap current and magnetic field-line curvature are found to take the same forms for both rotating and locked solutions. However, the term due to the perturbed ion polarization current can be different for rotating and locked solutions. In fact, the polarization term is usually stabilizing for freely rotating island chains, and usually destabilizing for locked island chains.

In Sec. V, we investigate the time evolution of an error-field-maintained magnetic island chain. The width of such a chain is forced to evolve on the same timescale as its phase. As before, there are two types of solutions: locked solutions and rotating solutions. Moreover, the locked solutions are such that the island chain is destabilized by the error-field. However, unlike the case of a pre-existing island chain, rotating solutions are found to have considerably smaller widths than locked solutions. Furthermore, there is significant hysteresis in the locking/unlocking process: i.e., once the error-field amplitude has exceeded the critical value required to convert a rotating solution into a locked solution, the amplitude must be decreased by a considerable factor in order to trigger the reverse transition. The width of a rotating error-field-maintained magnetic island chain pulsates in time, and periodically dips to zero. Moreover, the time evolution of the phase of a rotating error-field-maintained magnetic island chain is characterized by sudden phase jumps of π radians that occur each time the island width dips to zero. These jumps take place because it is impossible for an error-field-maintained island chain to exist in a certain range of phase relations with the error-field.

The time evolution of the toroidal ion fluid velocity associated with an error-field-maintained magnetic island chain is fairly similar to that of a pre-existing island chain, except that the fluid velocity inside the separatrix only shifts in the direction associated with island deceleration. As before, finite ion inertia introduces a time lag into the response of the toroidal ion fluid velocity to the acceleration of the island chain, and also gives rise to a perturbation of the toroidal ion fluid velocity many island widths distant from the island separatrix.

The analysis described in Sec. V has obvious relevance to ELM suppression experiments using deliberately applied, multi-harmonic, RMPs. In such experiments, the RMP is resonant at multiple rational surfaces, close to the edge of the plasma, which are all tearing stable. Now, the pedestal region of a conventional tokamak plasma is sufficiently hot that the widths of linear tearing layers are extremely small. In fact, the layer widths are so small that any detectible magnetic perturbation emanating from a rational surface almost certainly lies in the nonlinear regime in which the island width exceeds the linear layer width. Furthermore,

given that the rational surfaces in question are tearing stable, any magnetic islands driven at these surfaces must be maintained by the RMP. Thus, as long as the island chains driven at the various rational surfaces are forced to rotate with respect to the RMP, due to the action of plasma flow, their widths are suppressed considerably below the level expected by naively superposing the vacuum RMP onto the plasma equilibrium. The model traces shown in Figs. 7–9 are remarkably similar in form to the experimental traces reproduced in Fig. 29 of Ref. 33. This suggests that the experimental traces correspond to RMP-maintained rotating magnetic island chains, resonant at various different rational surfaces in the plasma pedestal, whose directions of rotation are the same as those at which naturally unstable island chains, resonant at the same rational surfaces, would propagate. Incidentally, the experimental data shown in Fig. 29 of Ref. 33, in which RMP-maintained magnetic island chains are forced to rotate, in an uneven fashion, by plasma rotation, can only be explained on the basis of nonlinear physics. The linear magnetic response of the plasma would be locked to the RMP, albeit with a phase-shift in the direction of the plasma rotation.³⁰ The width of a rotating RPM-supported magnetic island chain generated at a given rational surface by a given RMP scales as $|\omega_0|^{-1/3}$, where ω_0 is the natural frequency (i.e., the frequency of propagation of a naturally unstable island chain, with the same rational surface, in the absence of an RMP) defined in Eq. (74). This suggests that the driven width is particularly large if $|\omega_0| \simeq 0$ (although, $|\omega_0|$ cannot be too close to zero, otherwise the island chain will lock). Note, however, that the condition $|\omega_0| \simeq 0$ is not equivalent to the oft-quoted condition $|\omega_{\perp e}| \simeq 0$ (Ref. 34) (see Sec. IV C). The latter result is only valid in linear physics.

ACKNOWLEDGMENTS

This research was funded by the U.S. Department of Energy under Contract No. DE-FG02-04ER-54742.

APPENDIX: USEFUL DEFINITIONS

Let $k = [(1 + \Omega)/2]^{1/2}$. Then

$$\mathcal{A}(k < 1) \equiv 2k \langle 1 \rangle = \left(\frac{2}{\pi}\right) k K(k), \quad (\text{A1})$$

$$\mathcal{A}(k > 1) = \left(\frac{2}{\pi}\right) K\left(\frac{1}{k}\right), \quad (\text{A2})$$

$$\mathcal{B}(k > 1) \equiv \langle |X| \rangle = 1, \quad (\text{A3})$$

$$\mathcal{C}(k < 1) \equiv \frac{\langle X^2 \rangle}{2k} = \left(\frac{2}{\pi}\right) \frac{[E(k) + (k^2 - 1)K(k)]}{k}, \quad (\text{A4})$$

$$\mathcal{C}(k > 1) = \left(\frac{2}{\pi}\right) E\left(\frac{1}{k}\right), \quad (\text{A5})$$

$$\mathcal{D}(k > 1) \equiv \frac{\langle |X|^3 \rangle}{4k^2} = 1 - \frac{1}{2k^2}, \quad (\text{A6})$$

$$\begin{aligned} \mathcal{E}(k > 1) &\equiv \frac{\langle X^4 \rangle}{8k^3} \\ &= \left(\frac{2}{3\pi}\right) \left[2 \left(2 - \frac{1}{k^2}\right) E\left(\frac{1}{k}\right) - \left(1 - \frac{1}{k^2}\right) K\left(\frac{1}{k}\right) \right]. \end{aligned} \quad (\text{A7})$$

Here,

$$E(x) = \int_0^{\pi/2} (1 - x^2 \sin^2 u)^{1/2} du, \quad (\text{A8})$$

$$K(x) = \int_0^{\pi/2} (1 - x^2 \sin^2 u)^{-1/2} du \quad (\text{A9})$$

are standard complete elliptic integrals.

- ¹T. E. Evans, R. A. Moyer, K. H. Burrell, M. E. Fenstermacher, I. Joseph, A. W. Leonard, T. H. Osborne, G. D. Porter, M. J. Schaffer, P. B. Snyder, P. R. Thomas, J. G. Watkins, and W. P. West, *Nat. Phys.* **2**, 419 (2006).
- ²A. Kirk, E. Nardon, R. Akers, M. Bécoulet, G. De Temmerman, B. Dudson, B. Hnat, Y. Q. Liu, R. Martin, P. Tamain, D. Taylor, and MAST Team, *Nucl. Fusion* **50**, 034008 (2010).
- ³Y. Liang, P. Lomas, I. Nunes, M. Gryaznevich, M. N. A. Beurskens, S. Brezinsek, J. W. Coenen, P. Denner, T. Eich, L. Frassinetti, S. Gerasimov, D. Harting, S. Jachmich, A. Meigs, J. Pearson, M. Rack, S. Saarelma, B. Sieglin, Y. Yang, L. Zeng, and JET-EFDA Contributors, *Nucl. Fusion* **53**, 073036 (2013).
- ⁴Y. M. Jeon, J.-K. Park, S. W. Yoon, W. H. Ko, S. G. Lee, K. D. Lee, G. S. Yun, Y. U. Nam, W. C. Kim, J.-G. Kwak, K. S. Lee, H. K. Kim, and H. L. Yang, *Phys. Rev. Lett.* **109**, 035004 (2012).
- ⁵P. B. Snyder, R. J. Groebner, J. W. Hughes, T. H. Osborne, M. Beurskens, A. W. Leonard, H. R. Wilson, and X. Q. Xu, *Nucl. Fusion* **51**, 103016 (2011).
- ⁶M. R. Wade, R. Nazikian, J. S. de Grassie, T. E. Evans, N. M. Ferraro, R. A. Moyer, D. M. Orlov, R. J. Buttery, M. E. Fenstermacher, A. M. Garofalo, M. A. Lanctot, G. R. McKee, T. H. Osborne, M. A. Shafer, W. M. Solomon, P. B. Snyder, W. Suttrop, A. Wingen, E. A. Unterberg, and L. Zeng, *Nucl. Fusion* **55**, 023002 (2015).
- ⁷P. H. Rutherford, *Phys. Fluids* **16**, 1903 (1973).
- ⁸P. H. Rutherford, “Basic physical processes of toroidal fusion plasmas,” in *Proceedings of Course and Workshop*, Varenna, 1985 (Commission of the European Communities, 1986), Vol. 2, p. 531.
- ⁹R. Fitzpatrick and F. L. Waelbroeck, *Phys. Plasmas* **12**, 022307 (2005).
- ¹⁰R. Fitzpatrick and F. L. Waelbroeck, *Phys. Plasmas* **12**, 022308 (2005).
- ¹¹R. Fitzpatrick, P. G. Watson, and F. L. Waelbroeck, *Phys. Plasmas* **12**, 082510 (2005).
- ¹²R. Fitzpatrick, F. L. Waelbroeck, and F. Militello, *Phys. Plasmas* **13**, 122507 (2006).
- ¹³R. Fitzpatrick and F. L. Waelbroeck, *Phys. Plasmas* **14**, 122502 (2007).
- ¹⁴R. Fitzpatrick and F. L. Waelbroeck, *Phys. Plasmas* **15**, 012502 (2008).
- ¹⁵R. Fitzpatrick and F. L. Waelbroeck, *Phys. Plasmas* **16**, 072507 (2009).
- ¹⁶R. Fitzpatrick and F. L. Waelbroeck, *Plasma Phys. Controlled Fusion* **52**, 055006 (2010).
- ¹⁷R. Fitzpatrick and F. L. Waelbroeck, *Phys. Plasmas* **17**, 062503 (2010).
- ¹⁸R. Fitzpatrick, *Phys. Plasmas* **23**, 052506 (2016).
- ¹⁹R. Fitzpatrick, *Phys. Plasmas* **25**, 042503 (2018).
- ²⁰R. D. Hazeltine, M. Kotscheneuther, and P. J. Morrison, *Phys. Fluids* **28**, 2466 (1985).
- ²¹H. P. Furth, J. Killeen, and M. N. Rosenbluth, *Phys. Fluids* **6**, 459 (1963).
- ²²R. Fitzpatrick, *Nucl. Fusion* **33**, 1049 (1993).
- ²³J. A. Wesson, *Tokamaks*, 3rd ed. (Oxford University Press, 2004).
- ²⁴R. J. La Haye, C. C. Petty, E. J. Strait, F. L. Waelbroeck, and H. R. Wilson, *Phys. Plasmas* **10**, 3644 (2003).
- ²⁵P. Buratti, E. Alessi, M. Baruzzo, A. Casolari, E. Giovannozzi, C. Giroud, N. Hawkes, S. Menmuir, G. Purcella, and J. Contributors, *Nucl. Fusion* **56**, 076004 (2016).
- ²⁶Wolfram|Alpha, [http://www.wolframalpha.com/input/?i=integrate+x%5E4\(4*n-8\)%2F\(1%2Bx%5E4\)%5E4n](http://www.wolframalpha.com/input/?i=integrate+x%5E4(4*n-8)%2F(1%2Bx%5E4)%5E4n) for Wolfram Alpha LLC, 2009.

- ²⁷I. S. Gradshteyn and I. M. Ryzhik, *Table of Integrals, Series, and Products, Corrected and Enlarged Edition* (Academic Press, 1980), Eq. (3.613.1).
- ²⁸I. S. Gradshteyn and I. M. Ryzhik, *Table of Integrals, Series, and Products, Corrected and Enlarged Edition* (Academic Press, 1980), Eqs. (2.553.2) and (2.553.3).
- ²⁹A. J. Cole, C. C. Hegna, and J. D. Callen, *Phys. Rev. Lett.* **99**, 065001 (2007).
- ³⁰R. Fitzpatrick, *Phys. Plasmas* **5**, 3325 (1998).
- ³¹R. Fitzpatrick, *Plasma Phys. Controlled Fusion* **54**, 094002 (2012).
- ³²R. Fitzpatrick, *Phys. Plasmas* **21**, 092513 (2014).
- ³³R. Nazikian, C. C. Petty, A. Bortolon, X. Chen, D. Eldon, T. E. Evans, B. A. Grierson, N. M. Ferraro, S. R. Haskey, M. Knolker, C. Lasnier, N. C. Logan, R. A. Moyer, D. Orlov, T. H. Osborne, P. B. Synder, C. Paz-Soldan, F. Turco, H. Q. Wang, and D. H. Weisberg, "Grassy-ELM regime with edge resonant magnetic perturbations in fully noninductive plasmas in the DIII-D tokamak," *Nucl. Fusion* **58**, 106010 (2018).
- ³⁴N. M. Ferraro, T. E. Evans, L. L. Lao, R. A. Moyer, R. Nazikian, D. M. Orlov, M. W. Shafer, E. A. Unterberg, M. R. Wade, and A. Wingen, *Nucl. Fusion* **53**, 073042 (2013).